



## OPEN ACCESS

EDITED BY  
Shaochun Xu,  
Chinese Academy of Sciences (CAS), China

REVIEWED BY  
Shigeki Wada,  
University of Tsukuba, Japan  
Catherine Jane Collier,  
James Cook University, Australia

\*CORRESPONDENCE  
Neta Soto  
✉ [sotonet@post.bgu.ac.il](mailto:sotonet@post.bgu.ac.il)

RECEIVED 30 June 2023  
ACCEPTED 09 October 2023  
PUBLISHED 01 November 2023

## CITATION

Soto N, Winters G and Antler G (2023) The effect of anaerobic remineralization of the seagrass *Halophila stipulacea* on porewater biogeochemistry in the Gulf of Aqaba. *Front. Mar. Sci.* 10:1250931. doi: 10.3389/fmars.2023.1250931

## COPYRIGHT

© 2023 Soto, Winters and Antler. This is an open-access article distributed under the terms of the [Creative Commons Attribution License \(CC BY\)](https://creativecommons.org/licenses/by/4.0/). The use, distribution or reproduction in other forums is permitted, provided the original author(s) and the copyright owner(s) are credited and that the original publication in this journal is cited, in accordance with accepted academic practice. No use, distribution or reproduction is permitted which does not comply with these terms.

# The effect of anaerobic remineralization of the seagrass *Halophila stipulacea* on porewater biogeochemistry in the Gulf of Aqaba

Neta Soto<sup>1,2\*</sup>, Gidon Winters<sup>3,4</sup> and Gilad Antler<sup>1,2</sup>

<sup>1</sup>Department of Geological and Environmental Sciences, Ben-Gurion University of the Negev, Be'er Sheva, Israel, <sup>2</sup>The Interuniversity Institute for Marine Sciences, Eilat, Israel, <sup>3</sup>Dead Sea and Arava Science Center (DSASC), Masada National Park, Mount Masada, Israel, <sup>4</sup>Ben-Gurion University of the Negev, Eilat, Israel

**Introduction:** Seagrasses form oxidizing microenvironments around their roots, creating complex and strong redox gradients, thus affecting the rates of microbial carbon mineralization in their surrounding sediments. Since seagrasses are continuously being lost worldwide, a deeper understanding of the changes that occur within different seagrass sediments following the disappearance of the plants is of ecological and global importance.

**Methods:** We conducted a slurry experiment with sediments that have different characteristics from the northern tip of Gulf of Aqaba; the different sediments included different compartments of the tropical seagrass *Halophila stipulacea* (old and young leaves, rhizomes, or roots). We measured the changes over time in dissolved inorganic carbon (DIC), alkalinity, ferrous iron (Fe<sup>2+</sup>), hydrogen sulfide (H<sub>2</sub>S), sulfate (SO<sub>4</sub><sup>2-</sup>), and sulphur isotope ratios in sulfate within water. These measurements were used to calculate the rate of remineralization of each seagrass compartment, allowing us to predict the potential effects of the disappearance of different *H. stipulacea* compartments on key microbial processes in the surrounding environment.

**Results:** We show that *H. stipulacea*'s rhizomes had the fastest decomposition rates, followed by the young leaves, roots, and old leaves (which also indicates the preservation potential of old leaves).

**Discussion:** High concentrations of hydrogen sulfide were detected only in the slurries containing rhizomes and young leaves. High sulfide concentrations can lead to seagrass mortality and cause a positive feedback loop where the loss of seagrass due to sulfide generates further sulfide accumulation. This positive feedback loop can also be further reinforced by the loss of burrowing fauna in the sediment. This emphasizes the importance of understanding the extent of different pathways of seagrass disappearance on the surrounding environment and other geochemical feedbacks.

## KEYWORDS

*Halophila stipulacea*, Gulf of Aqaba (Eilat), sulfur, seagrass, blue carbon, sediments

## 1 Introduction

Seagrasses are highly productive marine flowering plants (angiosperms). They evolved from freshwater plants during at least three separate evolutionary events, the oldest of which is estimated to be around 100 million years ago (Les et al., 1997; Van Der Heide et al., 2012; Olsen et al., 2016). Worldwide, seagrasses can be found growing in shallow (0–50 m) coastal waters of all continents except Antarctica (Charpy-Roubaud and Sournia, 1990; Schubert and Demes, 2017; McKenzie et al., 2020). Seagrasses are usually found in soft sediments, where they may form dense meadows. Within these meadows, seagrass species diversity can vary from one dominant species to up to 14 species living in the same meadow (Short et al., 2007). Seagrass form complex habitats, provide extensive ecological services and due to their rich associated biodiversity, act as bioindicators of ecosystem health (Foden and Brazier, 2007; Marbà et al., 2015).

Seagrasses are also an efficient carbon sequestration ecosystem, and although they cover only 0.2% of the ocean floor, they are responsible for long-term storing 15% of carbon in the ocean (Laffoley and Grimsditch, 2009; Fourqurean et al., 2012; Mazarrasa et al., 2015). Once buried in the sediment, organic matter is oxidized to dissolved inorganic carbon (DIC) through the reduction of existing electron donors found in solid and dissolved phases. This process can be tracked by measuring the changes in pore water chemistry. The oxidation of organic matter

follows a sequence of terminal electron acceptors according to their Gibbs free energy yield, which is the largest energy yield associated with aerobic respiration. Once oxygen is depleted, microbes use nitrate ( $\text{NO}_3^-$ ) as the electron acceptor (denitrification is then followed by manganese and iron oxides reduction). The next reaction is the reduction of sulfate which uses aqueous  $\text{SO}_4^{2-}$  and produces hydrogen sulfide (here after “sulfide”). Finally, in the last reaction (methanogenesis), organic matter is converted into methane ( $\text{CH}_4$ ) by fermentation or by  $\text{CO}_2$  reduction (Froelich et al., 1979) (Figure 1). In marine and marginal marine sediments, microbial iron reduction accounts for about 10% of total sedimentary organic carbon oxidation, and microbial sulfate reductions are responsible for over 50% of organic carbon oxidation (Kasten and Jørgensen, 2000). These reactions are not always distinctly separated, and micro niches can be formed due to the actions of different organisms (e.g., burrowing organisms or roots), which interact with the sediment, breaking the delicate structure of the sedimentary sequence (e.g., Meysman et al., 2006).

The rhizosphere is the subsurface zone surrounding the rhizomes and roots. The biological and chemical properties of the sediment within the rhizosphere are affected by the roots present. The interaction of seagrasses with the surrounding sediment is complex (De Boer, 2007). Seagrasses release dissolved organic carbon (DOC) into the sediments, thus enriching the sediment with organic matter (Liu S et al., 2020; Sogin et al., 2022). This, in turn, promotes a series of microbial anaerobic respiration processes

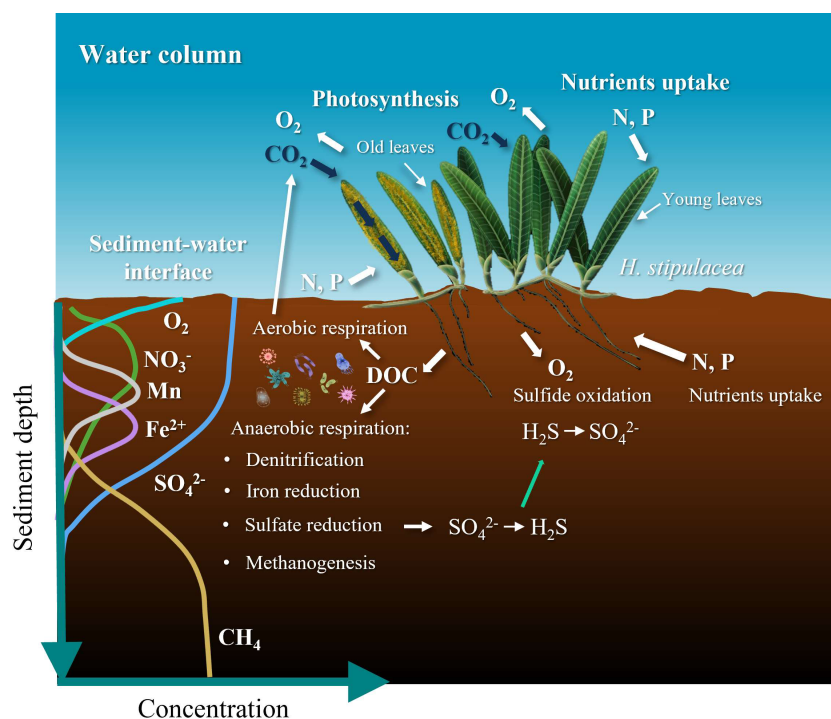


FIGURE 1

Illustration of the effect seagrass has on the chemistry of the surrounding sediments and water column; shown are also the profiles of terminal electron acceptors of inorganic compounds in organic matter oxidation as a redox depth gradient in sediments. Anaerobic respiration is the process which makes use of terminal electron acceptors other than oxygen. In general, the order of consumed oxidants is oxygen ( $\text{O}_2$ ) (aerobic respiration), followed by nitrate ( $\text{NO}_3^-$ ) and manganese (Mn) and Fe oxides and eventually sulfate ( $\text{SO}_4^{2-}$ ). Once sulfate is depleted, the dominant carbon metabolism pathway becomes methanogenesis. Based on Ugarelli et al., (2017).

in the sediment, including microbial iron reduction and microbial sulfate reduction to sulfide (Holmer et al., 2001; Calleja et al., 2007; Brodersen et al., 2017; Scholz et al., 2021). Sulfide is toxic to oxygen breathing- organisms and its penetration into seagrasses through their roots has been linked to seagrass mortality (Koch and Erskine, 2001; Lamers et al., 2013; Holmer and Hasler-Sheetal, 2014; Hasler-Sheetal and Holmer, 2015; Larkum et al., 2018; Fraser et al., 2023). Through their lacunae, seagrasses also transport oxygen to their roots, and once in the roots, this oxygen leaks out to the sediments that are generally depleted of oxygen within millimeters (Pedersen et al., 1998; Larkum et al., 2006). This pumping of oxygen into the rhizosphere creates a new micro-niche for other organisms and promotes aerobic respiration and sulfide oxidation which then converts the toxic sulfide to its less harmful oxidized form, sulfate ( $\text{SO}_4^{2-}$ ). Since coastal marine sediments are mostly anoxic, the microenvironment that seagrasses create by releasing oxygen through their roots is of major importance to burrowing organisms and particularly for the unique microbial communities that are associated with the root zone (e.g., Decho et al., 1985; Mateu-Vicens et al., 2010; Fales et al., 2020). Some of these bacterial communities in the rhizosphere are symbiotic and support the seagrass host by creating microenvironments that are beneficial to the seagrasses as well. One example being the sulfur oxidizing symbiotic bacteria found in the gills of burrowing lucinid clams (in seagrass sediments) which oxidize the toxic sulfide to sulfate (Van Der Heide et al., 2012; Cuccio et al., 2018; Martin et al., 2019). These interactions affect the fitness and health of the seagrasses themselves, but also the geochemistry of their surrounding sediments which have a tremendous impact on the carbon cycle (Devereux, 2005).

Seagrasses are threatened by global (e.g., global warming) and local (e.g., coastal development and eutrophication) stressors (Waycott et al., 2009). It is estimated that we have already lost 30% of historically known meadows, and since 1990 the rate of annual loss of seagrass worldwide is 7%. (e.g., Waycott et al., 2009; Lirman et al., 2014; Githaiga et al., 2019). Decline and loss of seagrass meadows is expected to have major consequences to coastal marine environments causing shifts of the primary producers in coastal areas and promotion of anoxic conditions in the sediments (Duarte, 2002). Loss of seagrass meadows will lead to a reduction in the capacity of worldwide seagrass meadows to sequester blue carbon, resulting in higher  $\text{CO}_2$  emissions to the water column and atmosphere through organic matter remineralization (or decomposition; the breakdown of organic carbon) in the sediments (Githaiga et al., 2019). Massive seagrasses die-offs could have two effects on the surrounding sediments (1) the dissolved oxygen released to the pore water by the seagrass roots will stop and (2) there is an addition of organic matter residue by the now dead seagrass (mostly the below-ground biomass). Both potential scenarios involved in seagrass die-offs, have been suggested to generate a positive feedback loop that will promote the generation of even more sulfide, which will then kill even more seagrasses (Lee and Dunton, 2000; Folmer et al., 2012; Hall et al., 2016; Maxwell et al., 2017).

*Halophila stipulacea* is a tropical seagrass and it is the dominant seagrass species in the Gulf of Aqaba. This is a relatively small

seagrass, characterized by leaves that are ~4-6 cm in length, short roots (~8 cm long) and horizontal elongation (Rotini et al., 2017). It is a strong, “weed-like”, fast growing, *r-strategist* species, which expands by producing dense patches (Boudouresque et al., 2009; Azcárate-García et al., 2020; Winters et al., 2020). In the Gulf of Aqaba, *H. stipulacea* can be found growing in a relatively wide range of conditions including different substrates - from fine sand to coral rubble (Lipkin, 1975; Rotini et al., 2017; Winters et al., 2017; Winters et al., 2020) and under different light environments - from high light environments (2m depth) to much lower light at deeper (>50 m) waters (Sharon et al., 2009). *H. stipulacea* can also be found in both anthropogenically disturbed and more pristine sites (Mejia et al., 2016).

The effect of the disappearance of the above-ground seagrass biomass on marine biogeochemical cycles in surrounding sediments might differ from the effect of losing both below- and above-ground biomasses. The remineralization rates and dynamics of different seagrass parts (e.g., leaves, roots, and rhizomes) depends on their biochemical composition, as well as the chemistry of the sediment they are exposed to (Berner, 1981; Jiang et al., 2010). Since seagrasses profoundly affect biogeochemical cycles and provide extensive ecological benefits, a deeper understanding of the temporal changes in sediments following the loss of above- and/or below-ground seagrass biomass is of ecological and global importance. However, the extent of such changes needs to be explored for different types of seagrass species, seagrass compartments, and with different sediments.

In this study, we simulated the dynamics of anaerobic remineralization of different *H. stipulacea* compartments in pore water chemistry of two different sediments from the Gulf of Aqaba. For this we performed slurry experiments by incubating sediments with filtered seawater and different seagrass parts for 25 days. We tracked the changes over time in water chemistry, dissolved inorganic carbon (DIC), alkalinity, sulfate, sulfide, ferrous iron, and sulfur isotope ratios in sulfate. The changes in these chemical species are indicative of the mechanism of microbial metabolism. To the best of our knowledge, this is the first time that decomposition rates of different seagrass compartments have been measured in a slurry incubation under anaerobic conditions.

## 2 Materials and methods

### 2.1 Study site

The study presented here took place at the Inter-University Institute for Marine Sciences (IUI; 29.502923N, 34.916450E; Eilat, Israel) close to the northern tip of the Gulf of Aqaba, an oligotrophic (nutrient-poor) basin located in the northern part of the Red Sea. The water column here is warm year-round (21-27°C) and oxygen-rich whilst the sediments are organic carbon poor with a content of  $\leq 0.6\%$  in uninfluenced areas (Blonder et al., 2017). Oxygen penetration depth in the sediment ranges from 3 mm in the sediment from ~20 m water depth to 20 mm in sediment from 700 m water depth (Boyko et al., 2018). The photic zone within the Gulf (>100 m water depth) is characterized by a primary production

range of 0.05–3.38 mg C m<sup>-3</sup> h<sup>-1</sup> (Levanon-Spanier et al., 1979; Stambler, 2006) which is limited in summer due to a nutrient (N, P) depletion (Reiss et al., 1984; Li et al., 1998).

We used natural sediments collected from *H. stipulacea* meadows growing in Eilat's north and south beaches (Figure 2A). Although the two sites are only 7 km away from each other, they differ from one another in several aspects (Mejia et al., 2016). The north beach has a moderate bathymetric slope (~2.7°), with fine sediment (most of which is between 63–250 µm), very few corals, and a continuous dense meadow (343,000 m<sup>2</sup> coverage area with a 60–100% seagrass density) starting from 1–2 m down to <30 m (Mejia et al., 2016; Winters et al., 2017). In this site, *H. stipulacea* meadows are exposed to a wide range of anthropogenic disturbances due to their proximity to tourist's beach strip, marina, and runoff from the Kinnet canal (Winters et al., 2017). In contrast, the south beach has a steeper bathymetric slope (~17.9°) (Mejia et al., 2016; Rotini et al., 2017), is exposed to minimal anthropogenic disturbances and runoff, and has a larger coral coverage and a small area covered in seagrass (61,900 m<sup>2</sup>, Winters et al., 2017). The sediment in the south beach is characterized by a relatively large grain size, with coarse sand-gravel/coral rubble (grain sizes of >2000 µm) (Mejia et al., 2016). Both the south and the north beach sediments contain relatively low amounts of total organic carbon (~0.5%) (Mejia et al., 2016).

## 2.2 Seagrass samples collection and handling

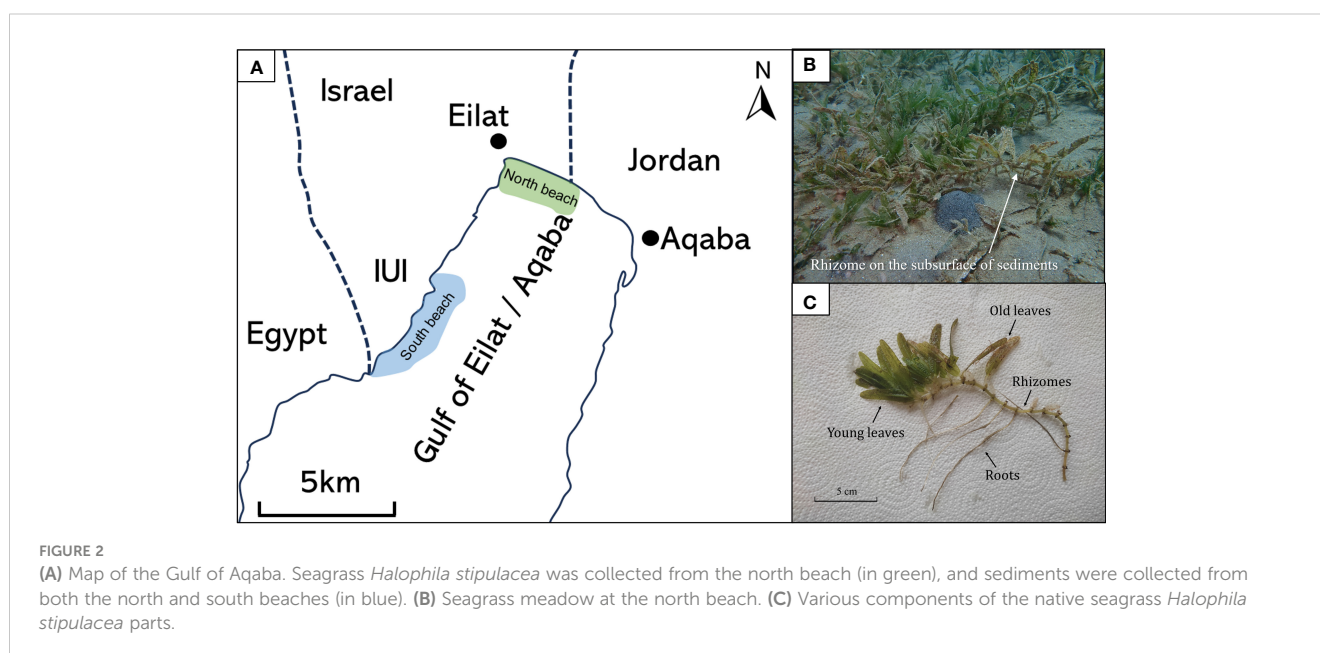
The seagrass samples for this study were collected during June 2022 from the north beach (29.544462N; 34.968831E) from 10 m depth (Figure 2A). Individual intact *H. stipulacea* plants (about a dozen individuals) were collected from the north beach site using SCUBA-diving (Permit #2023/43223; Israel Nature and Parks

Authority). Due to permit regulations, seagrass plants were only collected at the north beach site (an area that is not included in the local reserve). The plants were carefully removed from the sediment to avoid damage to the roots and rhizomes during the collection and transferred to ziplock bags filled with seawater. Within an hour post collection, the seagrasses were soaked in fresh water for one hour to remove detached fauna from the plant and salts, which affect the weight and the biochemical composition of the plant (previous work on *H. stipulacea* collected from the same sites showed no stress effect of such-short term exposures to low salinity; Oscar et al., 2018). Sand, epiphytes, and foraminifera were gently removed from the leaves, rhizome, and roots.

The seagrasses were then divided into different compartments: (1) the above-ground compartment, included both young - the green leaves - in the apical shoot, and (2) old leaves - the brown-yellowish leaves in the oldest shoot, alongside below-ground plant parts that included (3) rhizomes, and (4) roots. All samples were oven-dried for 24 hours (to stop any new biological activities). Subsequently, the seagrass parts were ground and sieved using a 125 µm sieve size and stored in a vacuum desiccator until the start of the experiment.

## 2.3 Sediment collection and preparation

Sediments were obtained from both the north and the south beaches (29.492291N; 34.906346E) by SCUBA-diving using 30 cm long transparent PVC tubes (i.e., sediment cores) with an internal diameter of 5 cm. From each location (south and north beaches), 5 separate sediment cores were collected adjacent to the seagrass meadows. Sediment cores were kept vertical to avoid any sediment disturbance. The water above the cores was filtered (0.22 µm) and flushed with N<sub>2</sub> (99.999%) gas for 2 hours, and this water was later added to the slurry.



## 2.4 Experimental setup and sampling

The upper 5 cm of sediments from within the sediment cores were collected within a few hours. The sediment was then placed in an N<sub>2</sub> (99.999%) pre-flushed Ziplock plastic bag and homogenized under a constant stream of N<sub>2</sub>. A total of 50 grams of homogenized sediment (wet weight) were then transferred to five new pre-flushed Ziplock plastic bags also filled with N<sub>2</sub>. The sediment was homogenized in the ziplock bag under a stream of N<sub>2</sub> that was manually kneaded for 10 minutes. To each bag, 0.5 grams of different dried and ground seagrass parts were added and mixed thoroughly for 20 minutes. Control sediment samples were treated in the same manner but without the addition of ground seagrass sample. Two grams of each mixture (sediment and plant parts) were then transferred to a serum bottle containing 10 ml of anoxic filtered seawater (0.22 μm) collected from the sediment core overlaying water. The serum bottles were filled to the top (with no head space), crimp-sealed with an aluminum cap and a butyl rubber stopper. Experiments were run as single-batch experiments, and duplicates were sacrificed for sampling at each time point. Overall, 20 single-batch reactors were used for each treatment (i.e., a total of 10 time points). In the south beach sediment experiment, the amount of old leaves was insufficient. Additionally, the amount of collected roots was enough for only one replicate (hence no duplicates). The laboratory experiment workflow is illustrated in Figure 3.

Water chemistry was monitored over 25 days at a sampling resolution of 1-3 days. The sampling interval was higher during the first 5 days and gradually decreased over time. At each sampling point water from the serum bottle was transferred to a syringe, filtered (0.22 μm), and immediately divided into different storage vials as follows: 0.9 ml of sample was mixed with 0.1 ml ferrozine for measuring ferrous iron concentration and stored at 4°C until measurement (Bialik et al., 2022). 0.1 ml of sample was mixed with 0.9 ml of ZnAc (0.05%) for sulfide measurement and stored in the freezer at -20°C until measurement (Pellerin et al., 2018). 0.9 ml of sample was mixed with 0.1 ml of ZnAc (4%) for sulfate and sulfur isotopes measurement and stored in -20°C until measurement (Pellerin et al., 2018). An additional 0.1 ml of sample was added to 5 ml of 2% nitric acid (HNO<sub>3</sub>) for measurement of major cations concentration and kept in the refrigerator until measurement (James et al., 2021). Alkalinity and dissolved inorganic carbon

(DIC) were measured immediately after sampling. The remaining sample was stored in the freezer at -20°C for nitrate measurement (Bialik et al., 2022).

## 2.5 Analytical methods

All water measurements were conducted in the NEGEV lab at The Interuniversity Institute of Eilat. Dissolved inorganic carbon (DIC) was measured using a DIC analyzer (AS-C6L, Apollo), which included a laser-based CO<sub>2</sub> detector (LI-7815, LI-COR, USA) (Lichtschlag et al., 2015). The precision of this method was less than 2 μM, resulting in less than 0.5% relative error (based on repeated measurement of each sample, n=5). Total alkalinity was measured using acid-base titration and calculated using a Gran plot. Samples were titrated with 0.005 M HCl which was calibrated by Dickson reference material (Batch #184). Titration was performed with an automated titrator (SI Analytics, Titroline 7000) with an average precision of 10 μEq/Kg (after James et al., 2021). Ferrous ions (Fe<sup>2+</sup>) were measured using the Ferrozine method with a spectrophotometer set to a wavelength of 562 nm (Agilent, Cary 8454) (Stookey, 1970). The detection limit of the Ferrozine assay is 1 μM and with a precision of 3%. Total sulfide concentrations were analyzed using a modified methylene blue assay (Cline, 1969) and measured by a spectrophotometer at a wavelength of 668 nm (Agilent, Cary 8454). The detection limit of the Cline's assay (Cline, 1969) is 1 μM and with a precision of 3%. Sulfate was measured by Ion Chromatography (Metrohm 930 Compact IC) with a precision better than 3% (Dick and Tabatabai, 1979). Major cations (Mn<sup>2+</sup>, Mg<sup>2+</sup>, Sr<sup>2+</sup>, Ca<sup>2+</sup>, K<sup>+</sup>, Na<sup>+</sup>) and dissolved Mn were analyzed by microwave plasma atomic emission spectrometer (MP-AES, Agilent) with a precision better than 3% (Balaram, 2020). Measurements were performed in duplicates. For δ<sup>34</sup>S<sub>SO4</sub> analysis, ZnAc (4%) was added first to precipitate sulfides. Following sample filtration (0.22 μm Sterile Syringe Filter), saturated BaCl<sub>2</sub> solution was added (1:1 ratio) to precipitate the sulfate as barite. The barite was subsequently rinsed with 6 N HCl acid and deionized water and set to dry at 50°C (after Antler et al., 2013). The dry barite was combusted at 1030°C in a Flash Element Analyzer (EA), and the resulting sulfur dioxide (SO<sub>2</sub>) was measured by continuous helium flow on a Continuous-Flow Isotope Ratio Mass Spectrometer (CF-IRMS Sercon, Integra wave) coupled to an Elemental Analyzer (Liu et al.,

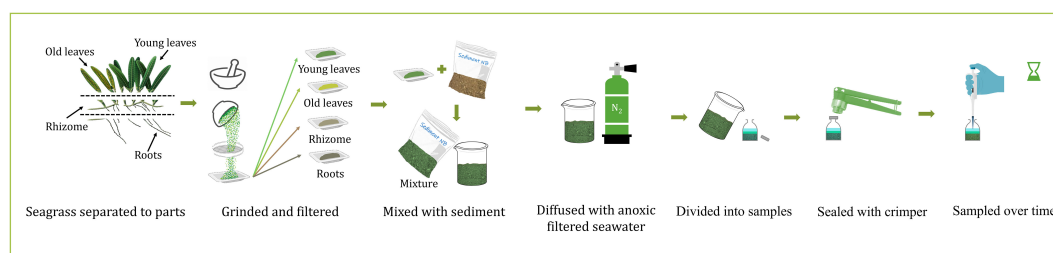


FIGURE 3

The experimental design. The collected *Halophila stipulacae* plants (Figure 2) were dried and then separated into above-ground compartments, i.e., old (yellowish-brown color) and young leaves (green color), and below-ground compartments, i.e., rhizomes and roots. Each part was then ground, filtered, and mixed with sediment and anoxic filtered seawater.

2021; 2022). The error was determined using the standard deviation of the standard NBS 127 at the beginning and at the end of each run ( $\sim 0.3\%$ ). Samples were corrected to NBS 127 ( $\delta^{34}\text{S}_{\text{SO}_4} = 21.1\%$ ). Carbon (C) and nitrogen (N) content in the seagrass were analyzed using a Continuous-Flow Isotope Ratio Mass Spectrometer (CF-IRMS Sercon, Integra wave) coupled to an Elemental Analyzer and were determined based on the integral of the  $\text{N}_2$  and  $\text{CO}_2$  peaks.

## 2.6 Rate calculations

Remineralization rates ( $\text{mM day}^{-1}$ ) were calculated based on the linear regression of the DIC vs. time plot (Equation 1):

$$\text{Rate} = \frac{\Delta\text{DIC}}{\Delta t} \quad \text{Eq.1}$$

Where Rate is the remineralization rates ( $\text{mM day}^{-1}$ ),  $\Delta\text{DIC}$  is the change in DIC (M) and  $\Delta t$  is the change in time (days). The rates were calculated based on a slope of a linear regression between each 3 consecutive time points (about 4–6 days). The error of these rate is reported as the standard errors of the slopes.

## 2.7 Sulfur isotopes and sulfur isotope fractionation calculation

Sulfur has four naturally occurring isotopes (with the relative abundances of each isotope shown in brackets):  $^{32}\text{S}$  (95.039%),  $^{33}\text{S}$  (0.748%),  $^{34}\text{S}$  (4.197%) and  $^{36}\text{S}$  (0.014%). Stable isotope ratios (e.g., for  $^{34}\text{S}$  over  $^{32}\text{S}$ ), are commonly reported using  $\delta$  notation, given as the following equation (Hoefs, 1997):

$$\delta^{34}\text{S}_{\text{SO}_4} = \left( \frac{R_{\text{Sample}}}{R_{\text{VCDT}}} - 1 \right) \quad \text{Eq.2}$$

where  $R = ^{34}\text{S}/^{32}\text{S}$ , and VCDT refers to the Vienna Canyon Diablo Troilite international reference scale.

Sulfur isotope fractionation factor ( $\epsilon$ ) was calculated from the regression of  $\delta^{34}\text{S}$  vs.  $-\ln(f)$  (Equation 3):

$$\delta^{34}\text{S}_{\text{SO}_4}(t) = \delta^{34}\text{S}_{\text{SO}_4}(0) - \epsilon \times \ln(f) \quad \text{Eq. 3}$$

where  $f$  is the fraction of reactant consumed relative to the initial amount of reactant (in this case sulfate),  $\delta^{34}\text{S}_{\text{SO}_4}(t)$  in permil ( $\text{‰}$ ) is the measured isotopic composition of the sulfate at time  $t$ ,  $\delta^{34}\text{S}_{\text{SO}_4}(0)$  is the initial isotopic composition of the sulfate and  $\epsilon$  is the isotope fractionation (in permil,  $\text{‰}$ ). Sulfur isotopes were measured only in the north beach sediment experiment.

## 2.8 Carbon loss calculation

The loss of organic carbon in the samples was calculated by the following manner (Equation 4):

$$\text{Carbon loss (\%)} = \frac{\Delta\text{DIC (M)} \cdot V \text{ (L)} \cdot \text{Mw(C)}}{\text{TOC (\%)} \cdot \text{Sw (g)}} \cdot 100 \quad \text{Eq. 4}$$

Where Carbon loss is the percent of organic carbon that was oxidized (%),  $\Delta\text{DIC}$  is the change in DIC (M) (DIC concentration the end of the experiment minus the DIC concentration at the beginning of the experiment),  $V$  is the serum bottle volume (L),  $\text{Mw}$  is the molar weight of carbon ( $\text{g}\cdot\text{mol}^{-1}$ ),  $\text{TOC}$  is the initial organic carbon fraction in the sediment, and  $\text{Sw}$  is the dry sediment weight.

## 3 Results

The changes in the concentrations of dissolved inorganic carbon (DIC), Alkalinity, ferrous iron ( $\text{Fe}^{2+}$ ), sulfide ( $\text{H}_2\text{S}$ ), sulfate ( $\text{SO}_4^{2-}$ ), and sulfur isotope ratios in sulfate  $\delta^{34}\text{S}_{\text{SO}_4}$  ( $\text{‰ VCDT}$ ) over time in sediments from the north and south beaches are presented in Figures 4, 5, respectively. The highest increase in DIC (Figures 4A, 5A) and alkalinity concentrations (Figures 4B, 5B) were detected in the rhizomes, followed by the young leaves, while the lowest increase was observed in the old leaves and roots, in both sites. In the rhizome group, DIC concentrations increased within 25 days from 2.1 mM (day 0) to 30.3 mM (day 25) in the north beach sediment, and from 2.1 mM (day 0) to 29.8 mM (day 25) in the south beach sediment. In the young leaves group, DIC concentrations increased from 2.2 mM (day 0) to 19.3 mM (day 14) in the north beach sediments and stayed relatively stable throughout the experiment (days 14–25). Similarly, DIC for the young leaves treatment exposed to the south beach sediments increased from 2.1 mM (day 0) to 20.7 mM (day 14) and stayed relatively stable in the south beach sediment bottles. In the old leaves group, DIC concentrations increased from 2.1 mM (day 0) to 11.2 mM (day 25) in the north beach (the old leaves group was not included in the south beach experiment – see section 2.2). In the roots group, DIC concentrations increased from 2.1 mM (day 0) to 11.2 mM (day 25) in the north beach sediments, and from 2 mM (day 0) to 9.5 mM (day 25) in the south beach sediments. Meanwhile, in the control group, DIC concentrations increased from 2.1 mM (day 0) to 4.1 mM (day 25) in the north beach sediments and from 2 mM (day 0) to 3.4 mM (day 25) in the south beach sediments.

In the rhizome group, alkalinity concentrations increased from 2.6  $\text{mEqKg}^{-1}$  (day 0) to 27.1  $\text{mEqKg}^{-1}$  (day 25) in the north beach sediments and from 2.6  $\text{mEqKg}^{-1}$  (day 0) to 28.1  $\text{mEqKg}^{-1}$  (day 25) in the south beach sediments. In the young leaves group, DIC concentrations increased from 2.8  $\text{mEqKg}^{-1}$  (day 0) to 19.4  $\text{mEqKg}^{-1}$  after 14 days in the north beach and stayed relatively stable throughout the rest of the experiment (until day 25) and increased from 2.9  $\text{mEqKg}^{-1}$  (day 0) to 21.2  $\text{mEqKg}^{-1}$  after 14 days and stayed relatively stable in the south beach sediments for the rest of the experiment (day 14–25). In the old leaves group, DIC concentrations increased from 2.8  $\text{mEqKg}^{-1}$  (day 0) to 11.5  $\text{mEqKg}^{-1}$  (day 25) in the north beach sediments. In the roots group, DIC concentrations increased from 2.5  $\text{mEqKg}^{-1}$  (day 0) to 11.2  $\text{mEqKg}^{-1}$  (day 25) in the north beach sediments and from 2.5  $\text{mEqKg}^{-1}$  (day 0) to 10.2  $\text{mEqKg}^{-1}$  (day 25) in the south beach sediments. In the control groups, DIC concentrations increased from 2.5  $\text{mEqKg}^{-1}$  (day 0) to 3.9  $\text{mEqKg}^{-1}$  (day 25) and from 2.5

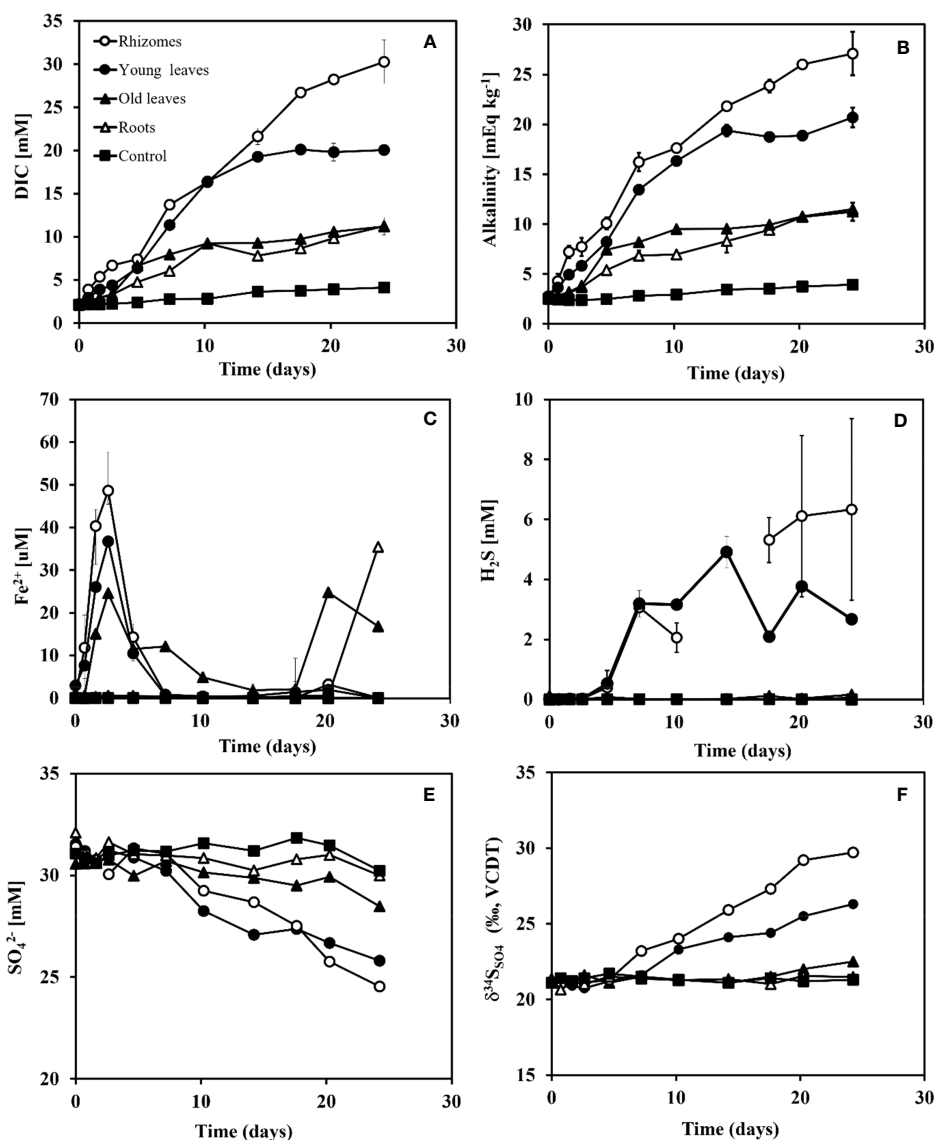


FIGURE 4

Changes in DIC, Alkalinity,  $\text{Fe}^{2+}$ ,  $\text{H}_2\text{S}$ ,  $\text{SO}_4^{2-}$  and  $\delta^{34}\text{S}_{\text{SO}_4}$  concentrations over time after adding different organic matter sources (i.e., different seagrass parts) to sediment taken from the north beach. Rhizomes in white dots, young leaves in black dots, roots in white triangles, old leaves in black triangles, and control in black squares. (A) DIC concentrations (mM), (B) Alkalinity concentrations ( $\text{mEq kg}^{-1}$ ), (C)  $\text{Fe}^{2+}$  concentrations ( $\mu\text{M}$ ), (D)  $\text{H}_2\text{S}$  concentrations ( $\mu\text{M}$ ), (E)  $\text{SO}_4^{2-}$  concentrations (mM) and (F)  $\delta^{34}\text{S}_{\text{SO}_4}$  (‰ VCDT) over time (days). Range bars at panels (A–D) represent the minimum and maximum values of the two replicates that were run ( $n=2$ ).

$\text{mEqKg}^{-1}$  (day 0) to  $3.4 \text{ mEqKg}^{-1}$  (day 25) in both the north and south beach sediments, respectively.

Ferrous iron ( $\text{Fe}^{2+}$ ) concentrations showed slight differences between the sediments from the two study sites (Figures 4C, 5C); while the trends are similar between the two types of sediments, the magnitude of  $\text{Fe}^{2+}$  changes are about five folds higher in the north beach sediments compared with south beach sediments.  $\text{Fe}^{2+}$  concentrations were highest in the rhizome group during the iron reduction phase, expressed by a peak in  $\text{Fe}^{2+}$  concentration ( $48.6 \mu\text{M}$ ) after 3 days in the north beach sediment and at  $7.8 \mu\text{M}$  after only 2 days in the south beach sediments. In the young leaves group,  $\text{Fe}^{2+}$  was highest after 3 days at  $36.7 \mu\text{M}$  in the north beach and at  $6.7 \mu\text{M}$  after 2 days in the south beach sediments. In the old leaves

group, two peaks in  $\text{Fe}^{2+}$  were recorded in the north beach; the first peak occurred after 3 days (at  $24.6 \mu\text{M}$ ) and the second peak occurred after 20 days (at  $24.8 \mu\text{M}$ ). In the roots group,  $\text{Fe}^{2+}$  concentration reached its highest level after 24 days in the sediments of the north beach ( $35.4 \text{ mM}$ ), whereas in the south beach sediments, it peaked after 4 days (at  $6 \text{ mM}$ ), decreased, and then increased again from  $6.3 \mu\text{M}$  (day 14) to  $16.4 \mu\text{M}$  (day 25). In control groups, no change in  $\text{Fe}^{2+}$  was recorded and concentrations remained at zero in sediments from both sites.

In sediments from the two sites, the highest increases in sulfide concentrations ( $\text{H}_2\text{S}$ ) were recorded in the rhizomes and young leaves groups (Figures 4D, 5D). In the rhizome group, sulfide increased from  $0 \text{ mM}$  (day 0) to  $6.3 \text{ mM}$  (day 25) in the north

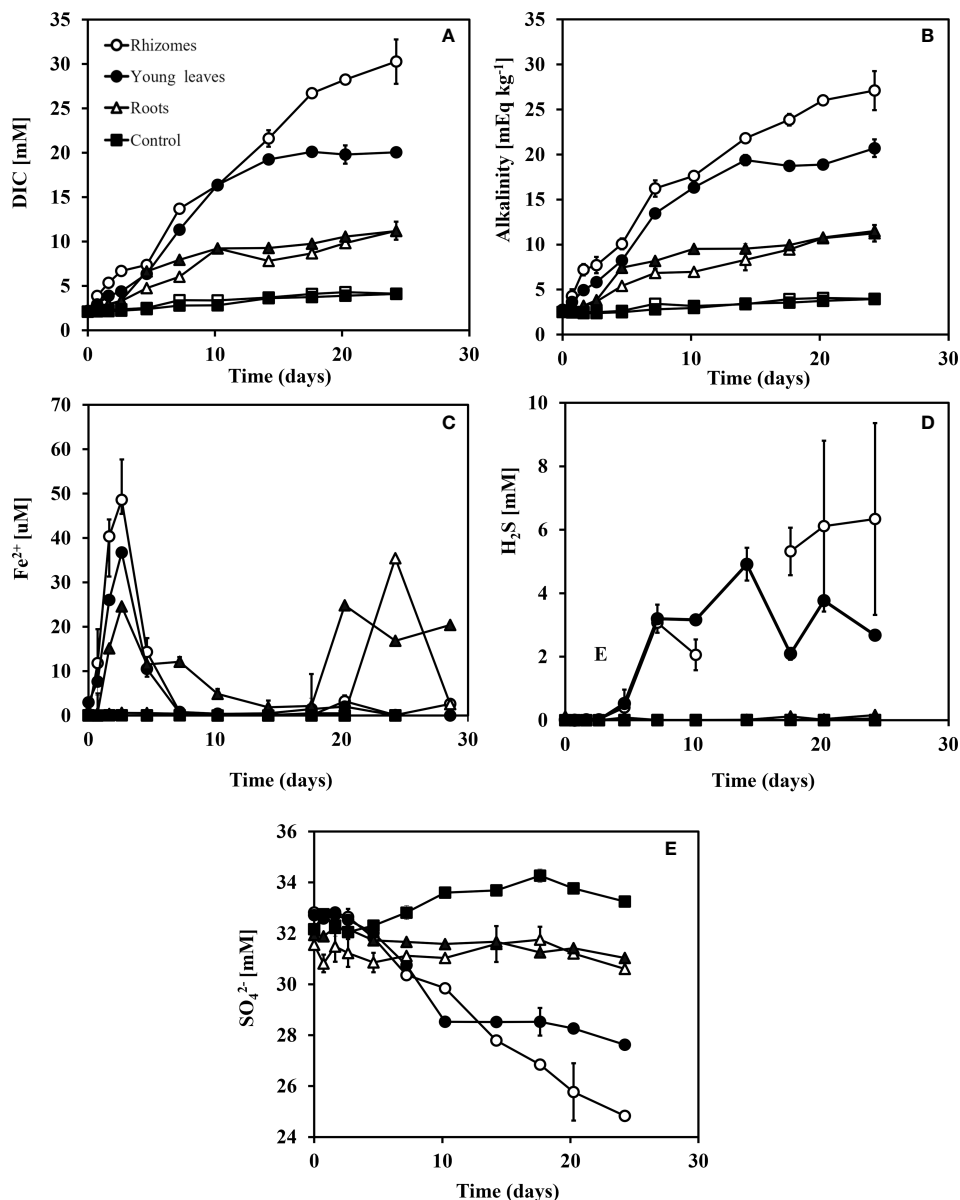


FIGURE 5

Changes in DIC, Alkalinity, Fe<sup>2+</sup>, H<sub>2</sub>S, SO<sub>4</sub><sup>2-</sup> and δ<sup>34</sup>S<sub>SO<sub>4</sub> concentrations over time after adding different organic matter sources (i.e., different seagrass parts) to sediment taken from the south beach. Rhizomes in white dots, young leaves in black dots, roots in white triangles, and control in black squares. (A) DIC concentrations (mM), (B) Alkalinity concentrations (mEq kg<sup>-1</sup>), (C) Fe<sup>2+</sup> concentrations (μM), (D) H<sub>2</sub>S concentrations (μM) and (E) SO<sub>4</sub><sup>2-</sup> concentrations (mM). Range bars at panels (A-D) represent the minimum and maximum values of the two replicates that were run (n=2).</sub>

beach sediments and from 0 (day 0) to 3.1 mM (day 25) in the south beach sediments. In the young leaves group, sulfide increased from 0 mM (day 0) to 3.2 mM after 7 days in the north beach sediments, and stayed relatively stable throughout the rest of the experiment (days 14-25) and increased from 0 (day 0) to 1.9 mM (day 25) in the south beach sediments. In the old leaves group, sulfide concentrations increased by only 0.1 mM at the north beach sediments. In the roots group, by the end of the experiment (day 25) sulfide had increased by only 0.2 mM in the north beach sediments and showed no change in the south beach sediments (0 mM).

The largest decreases in sulfate (SO<sub>4</sub><sup>2-</sup>) concentrations were recorded in the rhizome compartments, followed by the young leaves (Figures 4E, 5E). In the rhizome group, sulfate decrease from 32.8 mM (day 0) to 24.8 mM (day 25) in the north beach sediment and from 31.6 (day 0) to 26.9 mM (day 25) in the south beach sediments. In the young leaves group, sulfate decreased from 32.7 mM (day 0) to 28.5 mM after 10 days in the north beach sediment and stayed relatively stable throughout the experiment (days 10-25). Similarly, in the sediments from the south beach, sulfate decreased from 31.4 mM (day 0) to 28 mM (day 14) and remained stable (days 14-25). In the old leaves group, by the end of the experiment (day

25) sulfate concentrations had decreased by only 0.9 mM in the north beach. In the roots group, by the end of the experiment (day 25 compared to day 0) sulfide had increased by only 1 mM in sediments from both the north and south beaches. In the control groups, sulfide concentrations had increased by 1.1 mM and 1.2 mM (day 25 compared to day 0) in sediments from the north and south beaches, respectively.

This suggests that different seagrass parts remineralize at different rates, and that the products of this remineralization can vary in magnitude. Nitrate concentration and total dissolved Mn were lower than 0.3  $\mu\text{M}$  and 3  $\mu\text{M}$ , respectively in all samples (Tables S1-S9). Nitrate is the substrate for denitrification and from our results its concentration was low. Dissolved Mn concentration should increase during manganese reduction, yet this was not supported by our results which showed that Mn concentrations were less than 2  $\mu\text{M}$ , below the instrument detection limit (Tables S1-S9).  $\text{Ca}^{2+}$  concentrations were measured only in the north beach experiment.  $\text{Ca}^{2+}$  concentrations ranged from 10.6 to 11 mM in the young leaves group, from 11.1 to 11.5 mM in the old leaves group, from 10.8 to 11 mM in the rhizomes group, from 10.6 to 10.7 mM in the roots group and from 10.6 to 11 mM in the control group (Tables S1-S9). The standard deviation among all  $\text{Ca}^{2+}$  measurement is 0.3 mM ( $n=55$ ), which is even smaller than the analytical precision of this measurement (0.33 mM).

Since sulfur isotopes were measured only in the north beach sediment experiment, we could not compare between the two sediment types (Figure 4F). The sulfur isotope ratios in sulfate  $\delta^{34}\text{S}_{\text{SO}_4}$  (‰, VCDT) start with a seawater value of 21.1 ‰ and increased over time in sediments from the north beach, with the fastest increase found in the treatment that contained the rhizome compartment (29.7 ‰ after 24 days), followed by treatments that contained the young leaves group (26.1 ‰ after 24 days), with a small change over time in the old leaf group (22.5 ‰ after 24 days). Both the roots and control groups showed no change over time (standard deviation of 0.27 ‰ and 0.2 ‰ for the roots and control, respectively, which is lower than the instrument analytical precision). In the other groups (old leaves, roots and control) the

fractionation was not significantly different than zero ( $p$ -values are: 0.2 for the old leaves, 0.4 for the roots and 0.5 for the control).

Using the changes in DIC concentrations over time, the rates of remineralization were calculated during the experiment for both the north and south beaches sediments (Figure 6). These calculations showed that rhizomes had the highest remineralization rate among all groups in the first five days, followed by the young leaves and then the roots, old leaves, and the control. The rhizomes start at a faster remineralization rate (1.7  $\text{mM Day}^{-1}$ ) than the young leaves (0.8  $\text{mM Day}^{-1}$ ) and remain relatively stable (1.1  $\text{mM Day}^{-1}$ ) over time before their remineralization rates slowly decrease after 15 days to 0.5  $\text{mM Day}^{-1}$ . However, after day 5, the remineralization rates of young leaves bypassed that of the rhizomes and reached 1.8  $\text{mM Day}^{-1}$ . Although the remineralization rate of the leaves continued and actually bypassed the remineralization rate of the rhizomes between days 5 to 12 the amount of inorganic material released at the beginning was high enough to determine that the rhizome decomposed the fastest. The remineralization rate of the old leaves and roots was similar and lower than the young leaves and rhizomes for the entire duration of the experiment. In all experimental groups, the decomposition rates drop dramatically from day 10 (young leaves) or day 15 (rhizomes). Starting at 0.4  $\text{mM day}^{-1}$ , the rates of remineralization for roots in north beach sediments, drop already after 48 hours into the experiment.

When plotting the changes of DIC vs. alkalinity over time, most of the data points were found close to the 1:1 line at both sites (Figures 7A, C). At the north beach, the regression analysis for alkalinity vs. DIC yielded slopes of  $1.06 \pm 0.17$  ( $R^2 = 0.97$ ) (Figure 7A). The data from the south beach sediment yielded incredibly similar slopes of  $1.07 \pm 0.15$  (Figure 7C). However, overall, these slopes were not significantly different than 1 ( $p$ -value equals to 0.73 and 0.65,  $n=55$ , in the north and the south beach sediments, respectively). In sediments from both the north and south beaches, a significant increase in alkalinity concentration was recorded with little change in sulfate concentrations (Figures 7B, D). After sulfate concentrations started to decrease (during the sulfate reduction stage which started after five days) the alkalinity was doubled for every decrease in sulfate. The regression analysis for alkalinity vs. sulfate at the later stage of the

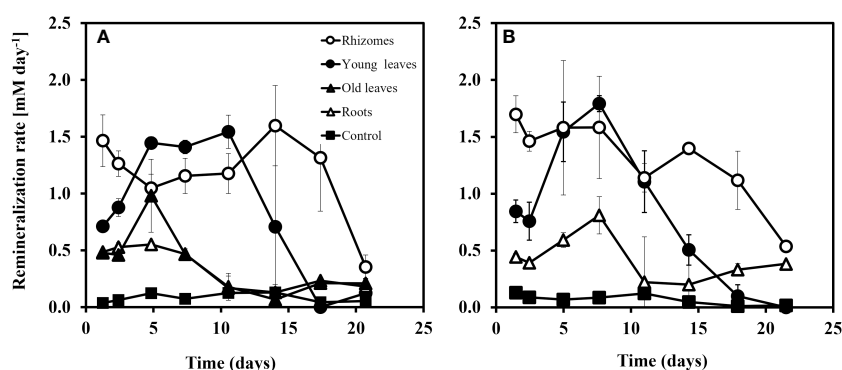
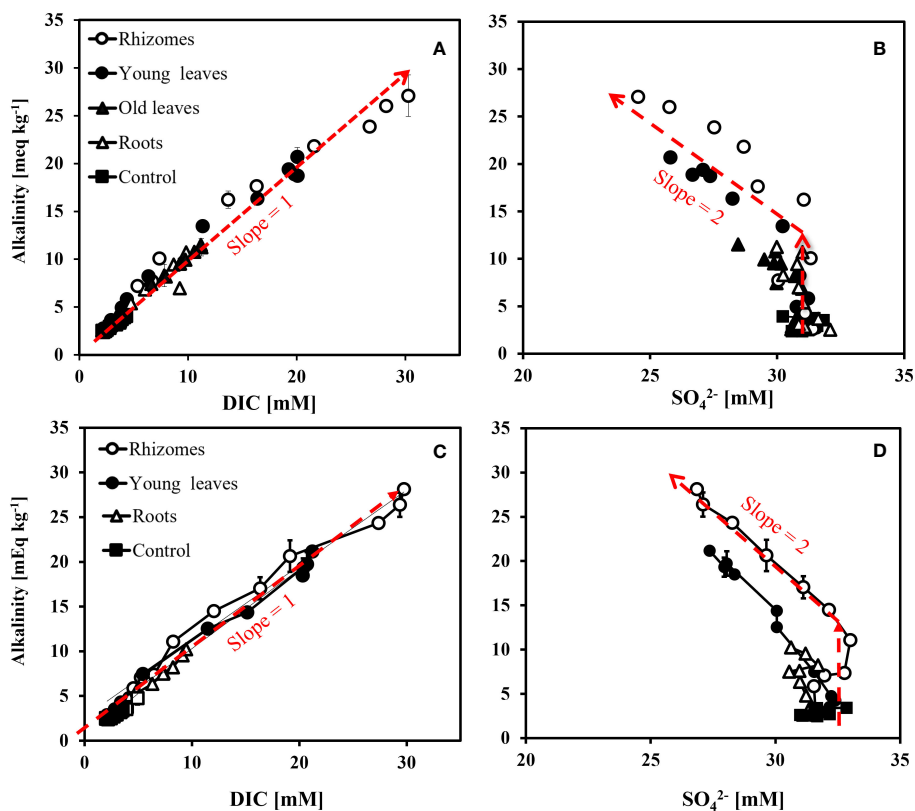


FIGURE 6

Remineralization rate ( $\text{mM day}^{-1}$ ) of the different seagrass parts in sediment from the north beach (A) and the south beach (B) at the Gulf of Aqaba. Rates were calculated based on the change (slope) of DIC vs. time. The error on the rates is given based on standard deviation of the slope ( $n=3-5$ ).



**FIGURE 7** Alkalinity vs. DIC concentrations change over time (A) and Alkalinity vs.  $\text{SO}_4^{2-}$  (B) from slurry with sediment from the north beach at the Gulf of Aqaba. Alkalinity vs. DIC concentrations change over time (C) and Alkalinity vs.  $\text{SO}_4^{2-}$  (D) from slurry with sediment from the south beach at the Gulf of Aqaba. The broken lines in the figure represent general trends rather than regression lines.

experiment (days 7-25), yielded slopes of  $-2.0 \pm 0.1$  ( $R^2 = 0.99$ ) for the rhizomes, and  $-2.2 \pm 0.5$  ( $R^2 = 0.92$ ) for the young leaves for the north beach. The regression analysis for alkalinity vs. sulfate resulted in slopes of  $-2.2 \pm 0.4$  ( $R^2 = 0.97$ , Rhizome) and  $-2.3 \pm 0.3$  ( $R^2 = 0.96$ , Young leaves) in the south beach. All these calculated slopes were not significantly different than -2 ( $p > 0.6$ ,  $n=11$ , in all experiments). The carbon (C) content was highest in the rhizomes ( $25.2\% \pm 0.8$ ) followed by the old leaves ( $23.3\% \pm 1.1$ ), roots ( $23.1\% \pm 0.8$ ) and finally the young leaves that had the lowest C content ( $22.3\% \pm 3.1$ ). The nitrogen (N) content however was highest in the young leaves ( $1.03\% \pm 0.14$ ) followed by the old leaves ( $0.47\% \pm 0.02$ ) and, rhizomes ( $0.47\% \pm 0.01$ ) and finally the roots with the lowest N content ( $0.46\% \pm 0.01$ ). The C:N ratios were  $53.3 \pm 1.6$  in the rhizomes,  $21.7 \pm 3.0$  in the young leaves,  $49.1 \pm 2.3$  in the old leaves and  $50.7 \pm 1.7$  in the roots (Table 1).

## 4 Discussion

### 4.1 Remineralization rates

Understanding the remineralization rates of different seagrass plant compartments may have implications for calculations of carbon stocks and sequestration rates. The remineralization rates in this study were calculated based on the DIC accumulation over time (Figures 4A, 5A) using equation 1 and shown in Figure 7. During the first 5 days of the experiment, in sediments from both the north and south beaches, the remineralization rates of the rhizomes were the highest followed by the remineralization rate of the young leaves (Figure 7).

A decrease in rates at the later stage of the experiment (starting at 7 to 15 days) was observed in all treatments, indicating a change

**TABLE 1** The average percentages ( $n=3$ ) of carbon (C) content, nitrogen (N) content and the C:N ratio in different seagrass compartments.

Treatment	C (%)	STD	N (%)	STD	C:N	STD
Young leaves	22.3	3.1	1.03	0.14	21.7	3.0
Old leaves	23.3	1.1	0.47	0.02	49.1	2.3
Rhizomes	25.2	0.8	0.47	0.01	53.3	1.6
Roots	23.1	0.8	0.46	0.01	50.7	1.7

SD refers to Standard Deviation.

of the remaining organic carbon quality. As the organic matter undergoes degradation, a noticeable decrease occurs in the labile fraction, accompanied by a decline in microbial activities rates (Holmer and Kristensen, 1994; Jørgensen et al., 2019).

The roots and the old leaves showed rather similar behavior, indicating their similarity in the recalcitrance of their organic carbon composition. Based on the changes in DIC and according to equation 4, we estimate the total loss of added organic carbon to be 50%, 30%, 15%, and 15% in the rhizome, young leaves, old leaves, and roots, respectively. These findings provide a significant insight for the estimation of seagrass carbon stocks and the possible impacts of seagrass decline on these stocks. The slow decomposition rate and low percentage of carbon loss in the roots compared to the young leaves and rhizomes, indicate that the below-ground biomass plays a critical role in the long-term carbon storage of seagrass meadows even while declining.

The remineralization rate is related to the biochemical composition of the different parts of the seagrass and is a proxy for their organic content. Previous work suggested that the C:N ratio of the organic matter is correlated with the decomposition rates (e.g., Enríquez et al., 1993). However, in *H. stipulacea* the C:N ratio appears to be highest in the rhizomes, followed by the roots and only then the leaves. This is shown both in our results (Table S1) and in a previous study (Beca-Carretero et al., 2019). This, somehow, contradicts our results as there is a mismatch between the relationship between the C:N ratio and the remineralization rates. Hence, the C:N ratio of the organic carbon by itself cannot be a proxy for the rates of decomposition. Similar observations were made in a recent study comparing the decomposition rates of seagrass compartments under aerobic conditions and showed that the above-ground biomass decomposed faster than the below-ground biomass (Satoh and Shigeki, 2022; Wada et al., 2022). This is likely since there are some labile (e.g., carbohydrates) and recalcitrant (e.g., lignin) organic components that have high C:N ratios. Therefore, in order to understand the remineralization rates of each seagrass part, a more detailed description of the seagrass biochemistry is needed.

While the biochemical characteristics of seagrass have been studied in the last several decades, most of that work took place in temperate seagrasses and sediments (Piñeiro-Juncal et al., 2022). In tropical seagrass species, it was found that in the Caribbean seagrass *Thalassia hemprichii*, the rhizomes had the highest concentration of sugars and starch followed by the leaves and then the roots, which concurs well with our experimental results. In *H. stipulacea*, a tropical species and the focus of this current study, it was found that the amount of starch and sucrose were higher in the rhizome than in the leaves (Helber et al., 2021). This could therefore suggest that a higher fraction of soluble sugars results in faster decomposition rates and a lower fraction of remaining organic carbon. Additionally, it is evident that there is a wide variation between the sugars content and organic matter between young and old roots (Waldron et al., 1989), which could explain why the decomposition rates of the old leaves showed more similarity towards the roots rather than the young leaves. Although in our study we separated between the leaves (according to their age, young vs old), we did not differentiate between the different age of roots since the root biomass was significantly lower

than other parts. It is also important to note that our experiments were run for 25 days, and it is possible that remineralization rates might show different trajectories at longer-time frames (months/years/decades). Since the decomposition rates in all groups decrease with time, we hypothesize that the remineralization rate would continue to be slower until all the non-refractory organic matter is consumed. As discussed earlier, we also do not expect the last reaction in the anaerobic respiration chain in sediments (i.e., methanogenesis) to occur as there is an excess of sulfate over organic carbon in our experiment.

## 4.2 Anaerobic microbial respiration dynamic

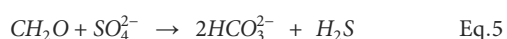
The slurry experiment method used in our study provides insights into the complex dynamics involved in the anaerobic remineralization of seagrass, as observed through changes in various water chemistry components (Chuan et al., 2020). In the absence of oxygen, a redox cascade of the main electron acceptors in the system (starting with denitrification, followed by manganese reduction, iron reduction, sulfate reduction and finally methanogenesis). These dynamics should be reflected in water chemistry. While we expect a decrease in the concentrations of the oxidizing species (such as  $\text{NO}_3^-$ , Mn and Fe oxides and  $\text{SO}_4^{2-}$ ) the concentrations of the reduced species should increase (such as  $\text{N}_2$ ,  $\text{NH}_4^+$ ,  $\text{Mn}^{2+}$ ,  $\text{Fe}^{2+}$ ,  $\text{H}_2\text{S}$ ,  $\text{CH}_4$ ). Our results indicate that organic matter remineralization primarily occurs through the reduction of iron oxides (after 3 days) and sulfate (after 5 days), while the remineralization occurring through nitrate ( $\text{NO}_3^-$ ) and Mn oxides are negligible (Tables S1–S9 and Figures 4, 5). This is in line with a previous observation from the Gulf of Aqaba and other oligotrophic environments showing that sulfate reduction is the dominant reaction in coastal sediments (Kristensen et al., 1998; Blonder et al., 2017). In addition, with such high sulfate concentrations, methane is not expected to be produced by acetolactic methanogenesis and/or by  $\text{CO}_2$  reduction (Sela-Adler et al., 2017). However, a recent study conducted on seagrass meadows of *Posidonia oceanica* revealed the occurrence of methane production during seagrass die-off from methylated compounds (Schorn et al., 2022).

Microbial iron reduction leads to an increase in dissolved ferrous iron concentrations, and microbial sulfate reduction results in a decrease in sulfate concentrations and a corresponding rise in dissolved sulfide (e.g., Jørgensen et al., 2019). Dissolved sulfide can react quickly with free dissolved ferrous iron to form iron monosulfide or pyrite (e.g., Pyzik and Sommer, 1981; Drobner et al., 1990). The results of our experiments (shown in Figures 4, 5) can be broadly divided into two stages: (1) microbial iron reduction dominates, and (2) microbial sulfate reduction becomes dominant. This dichotomy is particularly evident for the rhizomes and the young leaves treatments. The roots, old leaves, and the control treatments, seemed to be mostly dominated by bacterial iron reduction throughout the experiment while the rhizomes and young leaves treatments are dominated by microbial sulfate reduction.

The two study sites differ in their granulometry with the north beach sediment characterized by fine sediment (between 63–250  $\mu\text{m}$ ) while the south beach sediment is characterized by relatively large grain size (grain sizes of  $>2000 \mu\text{m}$ ) (Mejia et al., 2016). Bigger grain size will improve the conductivity between the seawater and pore water, which results in ventilation of the pore water. Surrounded by some of the driest deserts in the world, within the oligotrophic Gulf, much of the available nutrients that reaches the the sediment comes from airborne dust which impact many of the biological processes. Therefore, in our case, granulometry also implies on the mineralogy. Overall, there were no significant differences observed between sediments from the north and south beaches in most measurements (See correlation table; Table S12). The only major difference between the experiments were the results with ferrous iron concentrations, which can be attributed to differences in sediment source and the higher sedimentary reactive iron concentration in the north beach compared to the south beach sediments (Blonder et al., 2017; Boyko et al., 2019).

Although observations of biogeochemical trends over time provide valuable information, cross-plotting different components can enhance our understanding of reactions stoichiometries and provide a fresh perspective on the mechanism of microbial respiration. For instance, cross-plotting alkalinity vs. DIC indicates the mechanism of microbial respiration since it reflects the stoichiometry between the carbonate system species and proton donors (both of which change in a predictable way for each reaction in the sediment- Soetaert et al., 2007). Typically, microbial sulfate reduction produces one equivalent of alkalinity per one mole of DIC, while microbial iron reduction is closer to a ratio of one to eight (e.g., Soetaert et al., 2007). In our experiment, most Alkalinity vs. DIC data points fell close to 1:1 line (Figures 7A, C), suggesting a strong dominance of microbial sulfate reduction.

Evidence for the dominance of microbial sulfate reduction can also be gained by plotting the changes in alkalinity vs. the changes in sulfate concentrations over time. During microbial sulfate reduction, it is expected that for every loss of one sulfate molecule, two equivalents of alkalinity would be generated (e.g., Soetaert et al., 2007). Total Alkalinity expresses the balance between proton acceptors and proton donors in the solution (measured in equivalents per liter). Therefore, an addition of species such as bicarbonate ( $\text{HCO}_3^-$ ), carbonate ( $\text{CO}_3^{2-}$ ), bisulfide ( $\text{HS}^-$ ) and sulfide ( $\text{S}^{2-}$ ) will result in change in alkalinity. The oxidation of organic material by sulfate reduction follows the generalized reaction (Equation 5):



Hence, for a reduction of one mole of sulfate ( $\text{SO}_4^{2-}$ ) we anticipate an increase of 2 equivalents in alkalinity.

In this study, sediments from both the north and south beaches, showed a significant increase in alkalinity concentration over time, with little change in sulfate concentrations in the initial stage of our experiment (first five days). However, after sulfate concentrations started to decrease (during the sulfate reduction stage which started after five days) the alkalinity was doubled for every decrease in sulfate (Figures 7B, D). We suggest that the initial stage of the

incubations was dominated by bacterial iron reduction, yet during this stage we recorded a change of  $5\text{mEq kg}^{-1}$  of alkalinity (Figures 4, 5). However, iron increased by only  $50\mu\text{M}$  which can account only for a change of  $100\mu\text{Eq}$  of alkalinity (Figures 4B, C). In addition, this change in alkalinity was observed in both sediments from the north and south beaches while the iron reduction in the south beach was much less pronounced (Figures 4C, 5C). The lack of correlation between alkalinity and iron can be also demonstrated through a cross-plot (See Figure S1). Finally, other geochemical analysis revealed no significant change in  $\text{Ca}^{2+}$  concentrations (Tables S1–S9). This can indicate that no substantial dissolution of carbonate minerals occurred, which could have affected alkalinity without any change in sulfate concentration. As none of the measured inorganic chemical species could account for the initial stage's discrepancy in alkalinity mass balance, we suggest that the change was generated by fermentation and the production of organic alkalinity (e.g., the production of volatile fatty acids, Lukawska-Matuszewska, 2016).

This production of organic alkalinity in the form of volatile fatty acids could later fuel other microbial processes (Sansone and Martens, 1982; Glombitza et al., 2015). We assume that the volatile fatty acids formed in the first stage of the experiment were used by sulfate reducers as electron donor for microbial sulfate reduction (Glombitza et al., 2015). Taken together, we suggest that microbial iron reduction and fermentation, dominated the first 3–5 days of the experiment, followed by microbial sulfate reduction in the rhizome and young leaves (Figure 4) that took place in the later days of the experiment.

### 4.3 Microbial sulfate reduction dynamic

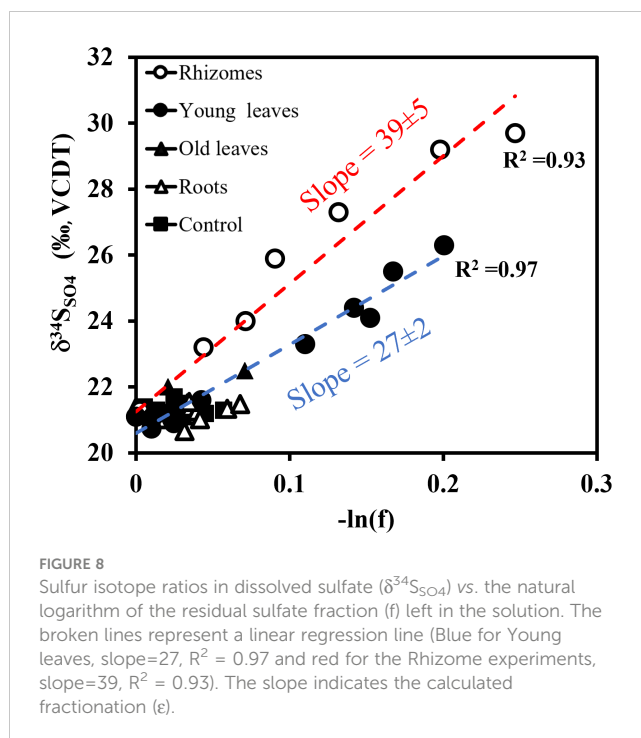
Sulfate is the second most abundant anion in the ocean with a concentration of  $32\text{mM}$  at the Gulf of Aqaba water column (e.g., Blonder et al., 2017). Therefore, microbial sulfate reduction plays a key role in the anaerobic remineralization of organic carbon in marine sediments (Jørgensen et al., 2019). Seagrass sediments exhibit relatively high rates of microbial sulfate reduction (Blackburn et al., 1994; Arnosti and Holmer, 1999; Holmer et al., 2001). In our experiments, the fastest decrease in sulfate concentrations were recorded in the slurry that included rhizomes, followed by the one that included young leaves. In comparison, the slurry that included roots or old leaves showed only a slight decrease, with the control staying relatively constant (Figure 4E). Similar observations were recorded in the south beach sediments (Figure 5). Correspondingly, the highest increase in sulfide concentrations were also measured in the rhizome and in the leaves, and with no detectable sulfide in the roots, old leaves, and control groups for seagrasses exposed to sediments from both sites (Figure 4D). These results suggest a strong dominance of microbial sulfate reduction with the rhizome and the young leaves and its absence in the roots.

Sulfur isotope ratios are a powerful tool to study microbial sulfate reduction. As microbial sulfate reduction progresses, the sulfur isotope composition of sulfate typically increases

monotonically (Harrison and Thode, 1958; Kaplan and Rittenberg, 1964; Rees, 1973). This is because the enzymatic steps tend to prefer the lighter sulfur isotope ( $^{32}\text{S}$ ) and leave behind the heavier  $^{34}\text{S}$ , resulting in the slow distillation of  $^{32}\text{S}$  into the external sulfide pool (Rees, 1973; Brunner and Bernasconi, 2005). The sulfur isotope fractionation ( $\epsilon$ ) during the microbial sulfate reduction can be as high as 72 ‰ (Wortmann et al., 2001; Brunner and Bernasconi, 2005; Sim et al., 2011a). The magnitude of sulfur isotope fractionation is influenced by factors such as microbial metabolism and carbon source, sulfate availability, temperature, and sulfate reduction rate (Brüchert, 2004; Brüchert et al., 2001; Canfield et al., 2006; Sim et al., 2011b; Antler et al., 2017; Pellerin et al., 2020). Furthermore, earlier studies found a positive correlation between the magnitude of sulfur isotope fractionation and sulfate reduction rate (Kaplan and Rittenberg, 1964; Rees, 1973; Chambers et al., 1975). This has been demonstrated in pure culture and batch culture experiments, as well as *in situ* using pore fluid profiles (Aharon and Fu, 2000; Canfield et al., 2006; Stam et al., 2011; Pellerin et al., 2020). Specifically, slower sulfate reduction rates corresponded to higher sulfur isotope fractionation (e.g., Leavitt et al., 2013; Wing and Halevy, 2014).

In our experiments, we found that sulfate reduction was only pronounced in the experiment with the rhizomes and the young leaves. The results showed a significant decrease in sulfate concentrations and an increase in sulfide and  $\delta^{34}\text{S}_{\text{SO}_4}$  (Figures 4D–F). To compare sulfur isotope enrichments among the experiments, the  $\delta^{34}\text{S}_{\text{SO}_4}$  was plotted against the natural logarithm of the ratio of the remaining sulfate (Figure 8). The faster  $\delta^{34}\text{S}_{\text{SO}_4}$  changes with the decreasing sulfate concentration, the larger the sulfur isotope enrichment or the isotope fractionation. Assuming Rayleigh-type fractionation in a closed system, the slope on this plot is the isotope fractionation ( $\epsilon$ ). The experiment with the addition of the rhizome part resulted in the highest sulfur isotope fractionation ( $39 \pm 5$  ‰) followed by the young leaves ( $27 \pm 2$  ‰) (See Figure 8). Other experiments did not produce a significant change in  $\delta^{34}\text{S}_{\text{SO}_4}$  that allowed us to calculate the sulfur isotope fractionation reliably. This provides further evidence of the different remineralization rates of these two parts, which is also consistent with our calculated rates (Figure 6). The fractionation was shown to be also dependent on the organic matter substrate, where an easier degradable substrate by microbes results in lower fractionation (Sim et al., 2011b; Pellerin et al., 2020; Antler et al., 2017).

Our results demonstrate that rhizomes and young leaves of *H. stipulacea* are rapidly remineralized in marine sediments, leading within a couple of days to the accumulation of high levels of toxic sulfide, a process that poses a risk to other seagrasses in the meadow. Furthermore, while both rhizomes and roots are commonly referred to as belowground biomass (Collier et al., 2021), our study suggest that their remineralization mechanism is different, possibly due to their different biochemical composition, which we predict will cause them to decompose at different rates, with the remineralization of rhizomes being faster than that of roots (Figure 6). The seagrass roots are typically embedded in the sediment depth, which is characterized by reduced oxygen levels, leading to the dominance of anaerobic reactions, yet our results show that the decomposition of the roots does not produce high



concentrations of sulfide, thus mitigating the risk of toxic sulfide intruding the roots of neighboring seagrasses and potentially killing them. The rhizomes, however, do yield high sulfide concentrations, yet their proximity to the sediment surface reduces the changes of sulfide reaching to deeper sediment layers where other seagrass roots are located. We therefore think it's important to distinguish between the roots and rhizomes.

## 5 Conclusions

Seagrass remineralization plays a critical role in the biogeochemistry of marine sediments, yet our understanding of the pathways of this remineralization is still limited. The decline of seagrasses is caused by a complex array of factors, including changes in water quality, eutrophication, climate change, coastal development, and overfishing (Jackson et al., 2001; Waycott et al., 2009; Holmer et al., 2011; Grech et al., 2012; Short et al., 2016). Organic matter enrichment in the sediments, which results in high sulfide concentrations was also found to be a major factor for seagrass decline (Carlson et al., 1994; Calleja et al., 2007; Folmer et al., 2012; Hall et al., 2016; Maxwell et al., 2017).

We conducted slurry experiments with sediments from the north and south beaches of the Gulf of Aqaba, sediments that differ in their granulometry, mineralogy and organic matter content, to investigate the effects of different plant compartments from the tropical seagrass *H. stipulacea* remineralization on sulfur, iron, and carbon biogeochemistry. Although our experiment represents a situation where seagrass parts are buried in their entirety, it can provide valuable insights into the pathways of seagrass remineralization in anoxic conditions. Our findings indicate that sulfide is generated only during the anaerobic remineralization of

young leaves and rhizomes, likely due to their biochemical composition. Notably, we did not observe high concentrations of sulfide during the anaerobic remineralization of roots, old leaves, or in the controls. This agrees with the remineralization rates of each seagrass plant part.

The sulfidic feedback loop, described as a positive feedback loop, where the generation of sulfide cause seagrass mortality, then, the remaining seagrass parts act as a substrate for sulfate reduction, resulting in generation of more sulfide. This positive feedback loop can also be further reinforced by the loss of burrowing fauna in the sediment such as mollusks and polychaetas and even lead to the production of methane (e.g., Wang and Chapman, 1999; Antler et al., 2019; Hutchings et al., 2019; van de Velde et al., 2020; Schorn et al., 2022). Seagrass increases oxygen concentration and pH levels in the water column (Job et al., 2023) and even enhances the resilience of coral reefs to ocean acidification (Unsworth et al., 2012; Lamb et al., 2017). Therefore, their decline may negatively affect neighboring ecosystems such as coral reefs (Waycott et al., 2009; Mollica et al., 2018). In *H. stipulacea*, the above-ground biomass to below-ground biomass ratio ranges between 0.5-1.5 (Beca-Carretero et al., 2020). Although the seagrass rhizome is considered part of the below-ground biomass, in *H. stipulacea* it is often seen protruding or laying on top of the sediment. Thus, the rhizome does not necessarily participate in anaerobic respiration processes in the sediment. Our results suggest that in the disappearance scenario of *H. stipulacea* at the Gulf of Aqaba, where only the above-ground biomass is removed while the roots remained anchored and decomposes in the sediment, the below-ground biomass (mainly roots) does not produce large quantities of sulfide. This may suggest that *H. stipulacea* die-offs might not result in a significant positive feedback loop in which decline of seagrass results in sulfide accumulation, causing further seagrass decline. This possible outcome highlights the importance of understanding the different pathways of seagrass remineralization.

Overall, the anaerobic remineralization rates of *H. stipulacea* below-ground biomass may also have implications for its potential long-term preservation and its role in carbon sequestration as a Blue Carbon ecosystem. Carbon dioxide removal from the atmosphere requires not only its fixation into organic form but also its burial, preferably in the sediment. Therefore, to store organic carbon in the sediment, the rates of remineralization of buried organic carbon must be low. Our findings suggest that *H. stipulacea*'s below-ground biomass exhibits a notably lower remineralization rate compared to the above-ground biomass, highlighting its potential as an effective carbon sink. Evidently, when the seagrass dies, the buried biomass within the sediment decomposes and releases DIC back to the water column at a slower phase. This decelerated decomposition pattern emphasizes *H. stipulacea*'s role as a substantial carbon sink, even while degrading.

It is important to note that our seagrass treatment and handling (cleaning, drying, and grinding) could have generated artifacts with respect to the chemical changes we detected (DIC, alkalinity,  $\text{Fe}^{2+}$ ,  $\text{SO}_4^{2-}$ ,  $\text{H}_2\text{S}$ ,  $\delta^{34}\text{S}_{\text{SO}_4}$  and major cations). For example, a possible change in the biochemical composition of the seagrass and loss of intracellular materials due to leaking caused by being soaked in

fresh water for an hour. However, no stress effect is expected from such short-term exposures to low salinity (Oscar et al., 2018). To prevent potential artifacts in future experiments, fauna could be removed under a stream of seawater and the seagrass samples could be washed under fresh water for a maximum of 5 minutes to remove salts.

Due to permit regulations, we were allowed to collect samples only from the north beach, making the amount of connected seagrass limiting; no "old leaves" were left for experiments with the south beach sediments, and the amount of roots was only sufficient for one replicate. In future experiments, we intend to request authorization and collocate a higher quantity of seagrasses. We also aim to replicate the conducted experiments using seagrass samples from the south beach and conduct the experiments under aerobic conditions as well. Seagrass samples can also be collected and examined in different seasons, to test possible effect of seasonally variable factors. Additionally, we intend to broaden the scope of the current study and repeat the experiment with other seagrass species. Despite the potential limitations to our method, there are still important insights we can make from such an experiment.

## Data availability statement

The original contributions presented in the study are included in the article/[Supplementary Material](#). Further inquiries can be directed to the corresponding author.

## Author contributions

NS, GW, and GA contributed to the conception and design of the study. NS and GA were involved in setting up the experiments, sediment and seagrass collection, and performing the chemical measurements. NS wrote the first draft of the manuscript. All authors contributed to the manuscript revision, read, and approved the submitted version.

## Funding

The author(s) declare financial support was received for the research, authorship, and/or publication of this article. The work was supported by Israel Science Foundation (2361/19).

## Acknowledgments

We would like to acknowledge Prof. Orit Sivan, Dr. Avner Gross and Dr. André Pellerin for the formative discussion that helped to shape this manuscript. We also would like to thank the two reviewers whose constructive comments immensely improved the quality of this manuscript. NS would like to thank Shany Barkan for her exceptional assistance in proofreading this manuscript.

## Conflict of interest

The authors declare that the research was conducted in the absence of any commercial or financial relationships that could be construed as a potential conflict of interest.

## Publisher's note

All claims expressed in this article are solely those of the authors and do not necessarily represent those of their affiliated

organizations, or those of the publisher, the editors and the reviewers. Any product that may be evaluated in this article, or claim that may be made by its manufacturer, is not guaranteed or endorsed by the publisher.

## Supplementary material

The Supplementary Material for this article can be found online at: <https://www.frontiersin.org/articles/10.3389/fmars.2023.1250931/full#supplementary-material>

## References

- Aharon, P., and Fu, B. (2000). Microbial sulfate reduction rates and sulfur and oxygen isotope fractionations at oil and gas seeps in deepwater Gulf of Mexico. *Geochimica Cosmochimica Acta* 64 (2), 233–246. doi: 10.1016/S0016-7037(99)00292-6
- Antler, G., Mills, J. V., Hutchings, A. M., Redeker, K. R., and Turchyn, A. V. (2019). The sedimentary carbon-sulfur-iron interplay—A lesson from East Anglian salt marsh sediments. *Front. Earth Sci.* 7, 140. doi: 10.3389/feart.2019.00140
- Antler, G., Turchyn, A. V., Ono, S., Sivan, O., and Bosak, T. (2017). Combined 34S, 33S and 18O isotope fractionations record different intracellular steps of microbial sulfate reduction. *Geochimica Cosmochimica Acta* 203, 364–380. doi: 10.1016/j.gca.2017.01.015
- Antler, G., Turchyn, A. V., Rennie, V., Herut, B., and Sivan, O. (2013). Coupled sulfur and oxygen isotope insight into bacterial sulfate reduction in the natural environment. *Geochimica Cosmochimica Acta* 118, 98–117. doi: 10.1016/j.gca.2013.05.005
- Arnosti, C., and Holmer, M. (1999). Carbohydrate dynamics and contributions to the carbon budget of an organic-rich coastal sediment. *Geochimica Cosmochimica Acta* 63 (3–4), 393–403. doi: 10.1016/S0016-7037(99)00076-9
- Azcárate-García, T., Beca-Carretero, P., Villamayor, B., Stengel, D. B., and Winters, G. (2020). Responses of the seagrass *Halophila stipulacea* to depth and spatial gradients in its native region (Red Sea): morphology, *in situ* growth and biomass production. *Aquat. Bot.* 165, 103252. doi: 10.1016/j.aquabot.2020.103252
- Balaram, V. (2020). Microwave plasma atomic emission spectrometry (MP-AES) and its applications—A critical review. *Microchemical J.* 159, 105483. doi: 10.1016/j.microc.2020.105483
- Beca-Carretero, P., Guihéneuf, F., Winters, G., and Stengel, D. B. (2019). Depth-induced adjustment of fatty acid and pigment composition suggests high biochemical plasticity in the tropical seagrass *Halophila stipulacea*. *Mar. Ecol. Prog. Ser.* 608, 105–117. doi: 10.3354/meps12816
- Berner, R. A. (1981). A new geochemical classification of sedimentary environments. *J. Sedimentary Res.* 51 (2), 359–365. doi: 10.1016/0016-7037(81)90164-2
- Bialik, O. M., Bookman, R., Elyashiv, H., Marietou, A., Saar, R., Rivlin, T., et al. (2022). Tropical storm-induced disturbance of deep-water porewater profiles, Gulf of Aqaba. *Mar. Geology* 453, 106926. doi: 10.1016/j.margeo.2022.106926
- Blackburn, T. H., Nedwell, D. B., and Wiebe, W. J. (1994). Active mineral cycling in a Jamaican seagrass sediment. *Marine Ecology Progress Series*, 233–239.
- Blonder, B., Boyko, V., Turchyn, A. V., Antler, G., Sinichkin, U., Knossow, N., et al. (2017). Impact of aeolian dry deposition of reactive iron minerals on sulfur cycling in sediments of the Gulf of Aqaba. *Front. Microbiol.* 8 1131. doi: 10.3389/fmicb.2017.01131
- Boudouresque, C. F., Bernard, G., Pergent, G., Shili, A., and Verlaque, M. (2009). Regression of Mediterranean seagrasses caused by natural processes and anthropogenic disturbances and stress: a critical review. *Botanica Marina* 52, 395–418. doi: 10.1515/BOT.2009.057
- Boyko, V., Blonder, B., and Kamysny, A. Jr. (2019). Sources and transformations of iron in the sediments of the Gulf of Aqaba (Red Sea). *Mar. Chem.* 216, 103691. doi: 10.1016/j.marchem.2019.103691
- Boyko, V., Torfstein, A., and Kamysny, A. (2018). Oxygen consumption in permeable and cohesive sediments of the Gulf of Aqaba. *Aquatic Geochemistry* 24, 165–193.
- Brüchert, V. (2004). Physiological and ecological aspects of sulfur isotope fractionation during bacterial sulfate reduction. *Geological Society of America* 379, 1–16. doi: 10.1130/0-8137-2379-5.1
- Brodersen, K. E., Koren, K., Mofßhammer, M., Ralph, P. J., and Santner, J. (2017). Seagrass-mediated phosphorus and iron solubilization in tropical sediments. *Environ. Sci. Technol.* 51 (24), 14155–14163. doi: 10.1021/acs.est.7b03878
- Brüchert, V., Knoblauch, C., and Jørgensen, B. B. (2001). Controls on stable sulfur isotope fractionation during bacterial sulfate reduction in Arctic sediments. *Geochimica Cosmochimica Acta* 65 (5), 763–776. doi: 10.1016/S0016-7037(00)00557-3
- Brunner, B., and Bernasconi, S. M. (2005). A revised isotope fractionation model for dissimilatory sulfate reduction in sulfate reducing bacteria. *Geochimica Cosmochimica Acta* 69 (20), 4759–4771. doi: 10.1016/j.gca.2005.04.015
- Calleja, M. L., Marbà, N., and Duarte, C. M. (2007). The relationship between seagrass (*Posidonia oceanica*) decline and sulfide porewater concentration in carbonate sediments. *Estuarine Coast. Shelf Sci.* 73 (3–4), 583–588. doi: 10.1016/j.ecss.2007.02.016
- Canfield, D. E., Olesen, C. A., and Cox, R. P. (2006). Temperature and its control of isotope fractionation by a sulfate-reducing bacterium. *Geochimica Cosmochimica Acta* 70 (3), 548–561. doi: 10.1016/j.gca.2005.10.028
- Carlson, J. P.R., Yarbrow, L. A., and Barber, T. R. (1994). Relationship of sediment sulfide to mortality of *Thalassia testudinum* in Florida Bay. *Bull. Mar. Sci.* 54 (3), 733–746.
- Chambers, L. A., Trudinger, P. A., Smith, J. W., and Burns, M. S. (1975). Fractionation of sulfur isotopes by continuous cultures of *Desulfovibrio desulfuricans*. *Can. J. Microbiol.* 21 (10), 1602–1607. doi: 10.1139/m75-234
- Charpy-Roubaud, C., and Sournia, A. (1990). The comparative estimation of phytoplanktonic, microphytobenthic and macrophytobenthic primary production in the oceans. *Mar. Microbial Food Webs* 4 (1), 31–57.
- Chuan, C. H., Gallagher, J. B., Chew, S. T., and Binti, M. Z. N. (2020). Blue carbon sequestration dynamics within tropical seagrass sediments: long-term incubations for changes over climatic scales. *Mar. Freshw. Res.* 71 (8), 892–904. doi: 10.1071/MF19119
- Cline, J. D. (1969). Spectrophotometric determination of hydrogen sulfide in natural waters 1. *Limnology Oceanography* 14 (3), 454–458. doi: 10.4319/lo.1969.14.3.0454
- Collier, C. J., Langlois, L. M., McMahon, K. M., Udy, J., Rasheed, M., Lawrence, E., et al. (2021). What lies beneath: Predicting seagrass below-ground biomass from above-ground biomass, environmental conditions and seagrass community composition. *Ecol. Indic.* 121, 107156. doi: 10.1016/j.ecolind.2020.107156
- Cucio, C., Overmars, L., Engelen, A. H., and Muyzer, G. (2018). Metagenomic analysis shows the presence of bacteria related to free-living forms of sulfur-oxidizing chemolithoautotrophic symbionts in the rhizosphere of the seagrass *Zostera marina*. *Front. Mar. Sci.* 5, 171. doi: 10.3389/fmars.2018.00171
- De Boer, W. F. (2007). Seagrass–sediment interactions, positive feedbacks and critical thresholds for occurrence: a review. *Hydrobiologia* 591, 5–24. doi: 10.1007/s10750-007-0780-9
- Decho, A. W., Hummon, W. D., and Fleeger, J. W. (1985). Meiofauna-sediment interactions around subtropical seagrass sediments using factor analysis. *J. Mar. Res.* 43 (1), 237–255. doi: 10.1357/002224085788437389
- Devereux, R. (2005). Seagrass rhizosphere microbial communities. Interactions Between Macro-and Microorganisms in Marine Sediments. *Coastal and Estuarine Studies* 60, 199–216. doi: 10.1029/CE060p199
- Dick, W. A., and Tabatabai, M. A. (1979). Ion chromatographic determination of sulfate and nitrate in soils. *Soil Sci. Soc. America J.* 43 (5), 899–904. doi: 10.2136/sssaj1979.03615995004300050016x
- Drobner, E., Huber, H., Wächtershäuser, G., Rose, D., and Stetter, K. O. (1990). Pyrite formation linked with hydrogen evolution under anaerobic conditions. *Nature* 346 (6286), 742–744. doi: 10.1038/346742a0
- Duarte, C. M. (2002). The future of seagrass meadows. *Environ. Conserv.* 29 (2), 192–206. doi: 10.1017/S0376892902000127
- Enriquez, S. C. M. D., Duarte, C. M., and Sand-Jensen, K. (1993). Patterns in decomposition rates among photosynthetic organisms: the importance of detritus C:N:P content. *Oecologia* 94, 457–471. doi: 10.1007/BF00566960

- Fales, R. J., Boardman, F. C., and Ruesink, J. L. (2020). Reciprocal interactions between bivalve molluscs and seagrass: a review and meta-analysis. *J. Shellfish Res.* 39 (3), 547–562. doi: 10.2983/035.039.0305
- Foden, J., and Brazier, D. P. (2007). Angiosperms (seagrass) within the EU water framework directive: a UK perspective. *Mar. Pollut. Bull.* 55 (1–6), 181–195. doi: 10.1016/j.marpolbul.2006.08.021
- Folmer, E. O., van der Geest, M., Jansen, E., Olff, H., Michael Anderson, T., Piersma, T., et al. (2012). Seagrass–sediment feedback: an exploration using a non-recursive structural equation model. *Ecosystems* 15, 1380–1393. doi: 10.1007/s10021-012-9591-6
- Fourqurean, J. W., Duarte, C. M., Kennedy, H., Marbà, N., Holmer, M., Mateo, M. A., et al. (2012). Seagrass ecosystems as a globally significant carbon stock. *Nat. Geosci.* 5 (7), 505–509. doi: 10.1038/ngeo1477
- Fraser, M. W., Martin, B. C., Wong, H. L., Burns, B. P., and Kendrick, G. A. (2023). Sulfide intrusion in a habitat forming seagrass can be predicted from relative abundance of sulfur cycling genes in sediments. *Sci. Total Environ.* 864, 161144. doi: 10.1016/j.scitotenv.2022.161144
- Froelich, P., Klinkhammer, G. P., Bender, M. L., Luedtke, N. A., Heath, G. R., Cullen, D., et al. (1979). Early oxidation of organic matter in pelagic sediments of the eastern equatorial Atlantic: suboxic diagenesis. *Geochimica cosmochimica Acta* 43 (7), 1075–1090. doi: 10.1016/0016-7037(79)90095-4
- Githaiga, M. N., Frouws, A. M., Kairo, J. G., and Huxham, M. (2019). Seagrass removal leads to rapid changes in fauna and loss of carbon. *Front. Ecol. Evol.* 7, 62. doi: 10.3389/fevo.2019.00062
- Glombitza, C., Jaussi, M., Roy, H., Seidenkrantz, M. S., Lomstein, B. A., and Jørgensen, B. B. (2015). Formate, acetate, and propionate as substrates for sulfate reduction in sub-arctic sediments of Southwest Greenland. *Front. Microbiol.* 6, 846. doi: 10.3389/fmicb.2015.00846
- Grech, A., Chartrand-Miller, K., Erfemeijer, P., Fonseca, M., McKenzie, L., Rasheed, M., et al. (2012). A comparison of threats, vulnerabilities and management approaches in global seagrass bioregions. *Environ. Res. Lett.* 7 (2), 024006. doi: 10.1088/1748-9326/7/2/024006
- Hall, M. O., Furman, B. T., Merello, M., and Durako, M. J. (2016). Recurrence of *Thalassia testudinum* seagrass die-off in Florida Bay, USA: initial observations. *Mar. Ecol. Prog. Ser.* 560, 243–249. doi: 10.3354/meps11923
- Harrison, A. G., and Thode, H. G. (1958). Mechanism of the bacterial reduction of sulphate from isotope fractionation studies. *Trans. Faraday Soc.* 54, 84–92. doi: 10.1039/tf9585400084
- Hasler-Sheetal, H., and Holmer, M. (2015). Sulfide intrusion and detoxification in the seagrass *Zostera marina*. *PLoS One* 10 (6), e0129136. doi: 10.1371/journal.pone.0129136
- Helber, S. B., Winters, G., Stuhr, M., Belshe, E. F., Bröhl, S., Schmid, M., et al. (2021). Nutrient history affects the response and resilience of the tropical seagrass *Halophila stipulacea* to further enrichment in its native habitat. *Front. Plant Sci.* 12, 678341. doi: 10.3389/fpls.2021.678341
- Hoefs, J. (1997). *Stable isotope geochemistry* Vol. 201 (Berlin: Springer).
- Holmer, M., Andersen, F. Ø., Nielsen, S. L., and Boschker, H. T. (2001). The importance of mineralization based on sulfate reduction for nutrient regeneration in tropical seagrass sediments. *Aquat. Bot.* 71 (1), 1–17. doi: 10.1016/S0304-3770(01)00170-X
- Holmer, M., and Hasler-Sheetal, H. (2014). Sulfide intrusion in seagrasses assessed by stable sulfur isotopes—a synthesis of current results. *Front. Mar. Sci.* 1, 64. doi: 10.3389/fmars.2014.00064
- Holmer, M., and Kristensen, E. (1994). Coexistence of sulfate reduction and methane production in an organic-rich sediment. *Marine Ecology-Progress Series* 107, 177–177.
- Holmer, M., Wirachwong, P., and Thomsen, M. S. (2011). Negative effects of stress-resistant drift algae and high temperature on a small ephemeral seagrass species. *Mar. Biol.* 158, 297–309. doi: 10.1007/s00227-010-1559-5
- Hutchings, A. M., Antler, G., Wilkening, J. V., Basu, A., and Bradbury, H. J. (2019). Creek dynamics determine pond subsurface geochemical heterogeneity in east anglian (uk) salt marshes. *Front. Earth Sci.* 7, 41. doi: 10.3389/feart.2019.00041
- Jackson, J. B., Kirby, M. X., Berger, W. H., Bjørndal, K. A., Botsford, L. W., Bourque, B. J., et al. (2001). Historical overfishing and the recent collapse of coastal ecosystems. *science* 293 (5530), 629–637.
- James, D. H., Bradbury, H. J., Antler, G., Steiner, Z., Hutchings, A. M., Sun, X., et al. (2021). Assessing sedimentary boundary layer calcium carbonate precipitation and dissolution using the calcium isotopic composition of pore fluids. *Front. Earth Sci.* 9, 601194. doi: 10.3389/feart.2021.601194
- Jiang, Z. J., Huang, X. P., and Zhang, J. P. (2010). Effects of CO<sub>2</sub> enrichment on photosynthesis, growth, and biochemical composition of seagrass *Thalassia hemprichii* (Ehrenb.) Aschers. *J. Integr. Plant Biol.* 52 (10), 904–913. doi: 10.1111/j.1744-7909.2010.00991.x
- Job, S., Sekadende, B., Yona, G., George, R., Lugendo, B. R., and Kimirei, I. A. (2023). Effect of seagrass cover loss on seawater carbonate chemistry: Implications for the potential of seagrass meadows to mitigate ocean acidification. *Regional Stud. Mar. Sci.* 60, 102816. doi: 10.1016/j.rsma.2023.102816
- Jørgensen, B. B., Findlay, A. J., and Pellerin, A. (2019). The biogeochemical sulfur cycle of marine sediments. *Front. Microbiol.* 10, 849. doi: 10.3389/fmicb.2019.00849
- Kaplan, I. R., and Rittenberg, S. C. (1964). Microbiological fractionation of sulphur isotopes. *Microbiology* 34 (2), 195–212. doi: 10.1099/00221287-34-2-195
- Kasten, S., and Jørgensen, B. B. (2000). Sulfate reduction in marine sediments. *Mar. geochemistry*, 263–281. doi: 10.1007/978-3-662-04242-7\_8
- Koch, M. S., and Erskine, J. M. (2001). Sulfide as a phytotoxin to the tropical seagrass *Thalassia testudinum*: interactions with light, salinity and temperature. *J. Exp. Mar. Biol. Ecol.* 266 (1), 81–95. doi: 10.1016/S0022-0981(01)00339-2
- Kristensen, E., Jensen, M. H., Banta, G. T., Hansen, K., Holmer, M., and King, G. M. (1998). Transformation and transport of inorganic nitrogen in sediments of a southeast Asian mangrove forest. *Aquat. Microbial Ecol.* 15 (2), 165–175. doi: 10.3354/ame015165
- Laffoley, D., and Grimsditch, G. D. (2009). The management of natural coastal carbon sinks. *Iucn*, 23–29. doi: 10.1007/978-3-319-71354-0
- Lamb, J. B., Van De Water, J. A., Bourne, D. G., Altier, C., Hein, M. Y., Fiorenza, E. A., et al. (2017). Seagrass ecosystems reduce exposure to bacterial pathogens of humans, fishes, and invertebrates. *Science* 355 (6326), 731–733. doi: 10.1126/science.aal1956
- Lamers, L. P., Govers, L. L., Janssen, I. C., Geurts, J. J., van der Welle, M. E., Van Katwijk, M. M., et al. (2013). Sulfide as a soil phytotoxin—a review. *Front. Plant Sci.* 4, 268. doi: 10.3389/fpls.2013.00268
- Larkum, A. W., Kendrick, G. A., and Ralph, P. J. (Eds.) (2018). *Seagrasses of Australia: structure, ecology and conservation* (Springer International Publishing AG).
- Larkum, A. W., Orth, R. J., Duarte, C. M., Borum, J., Sand-Jensen, K., Binzer, T., et al. (2006). Oxygen movement in seagrasses. *Seagrasses: biology ecology and Conserv.* 255–270.
- Leavitt, W. D., Halevy, I., Bradley, A. S., and Johnston, D. T. (2013). Influence of sulfate reduction rates on the Phanerozoic sulfur isotope record. *Proc. Natl. Acad. Sci.* 110 (28), 11244–11249. doi: 10.1073/pnas.1218874110
- Lee, K. S., and Dunton, K. H. (2000). Diurnal changes in pore water sulfide concentrations in the seagrass *Thalassia testudinum* beds: the effects of seagrasses on sulfide dynamics. *J. Exp. Mar. Biol. Ecol.* 255 (2), 201–214. doi: 10.1016/S0022-0981(00)00300-2
- Les, D. H., Cleland, M. A., and Waycott, M. (1997). Phylogenetic studies in Alismatidae. II: evolution of marine angiosperms (seagrasses) and hydrophyly. *Systematic Bot.* 22, 443–463. doi: 10.2307/2419820
- Levanon-Spanier, I., Padan, E., and Reiss, Z. (1979). Primary production in a desert-enclosed sea—the Gulf of Elat (Aqaba), Red Sea. *Deep Sea Res. Part A. Oceanographic Res. Papers* 26 (6), 673–685. doi: 10.1016/0198-0149(79)90040-2
- Li, H., Veldhuis, M. J., and Post, A. F. (1998). Alkaline phosphatase activities among planktonic communities in the northern Red Sea. *Mar. Ecol. Prog. Ser.* 173, 107–115. doi: 10.3354/meps173107
- Lichtsschlag, A., James, R. H., Stahl, H., and Connelly, D. (2015). Effect of a controlled sub-seabed release of CO<sub>2</sub> on the biogeochemistry of shallow marine sediments, their pore waters, and the overlying water column. *Int. J. Greenhouse Gas Control* 38, 80–92. doi: 10.1016/j.ijggc.2014.10.008
- Lipkin, Y. (1975). *Halophila stipulacea*, a review of a successful immigration. *Aquat. Bot.* 1, 203–215. doi: 10.1016/0304-3770(75)90023-6
- Lirman, D., Thyberg, T., Santos, R., Schopmeyer, S., Drury, C., Collado-Vides, L., et al. (2014). SAV communities of western Biscayne Bay, Miami, Florida, USA: Human and natural drivers of seagrass and macroalgae abundance and distribution along a continuous shoreline. *Estuaries coasts* 37, 1243–1255. doi: 10.1007/s12237-014-9769-6
- Liu, S., Deng, Y., Jiang, Z., Wu, Y., Huang, X., and Macreadie, P. I. (2020). Nutrient loading diminishes the dissolved organic carbon drawdown capacity of seagrass ecosystems. *Sci. Total Environ.* 740, 140185. doi: 10.1016/j.scitotenv.2020.140185
- Liu, J., Antler, G., Pellerin, A., Izon, G., Dohrmann, I., Findlay, A. J., et al. (2021). Isotopically “heavy” pyrite in marine sediments due to high sedimentation rates and non-steady-state deposition. *Geology* 49 (7), 816–821. doi: 10.1130/G48415.1
- Liu, J., Pellerin, A., Wang, J., Rickard, D., Antler, G., Zhao, J., et al. (2022). Multiple sulfur isotopes discriminate organoclastic and methane-based sulfate reduction by seafloor pyrite formation. *Geochimica et Cosmochimica Acta* 316, 309–330. doi: 10.1016/j.gca.2021.09.026
- Lukawska-Matuszewska, K. (2016). Contribution of non-carbonate inorganic and organic alkalinity to total measured alkalinity in pore waters in marine sediments (Gulf of Gdansk, SE Baltic Sea). *Mar. Chem.* 186, 211–220. doi: 10.1016/j.marchem.2016.10.002
- Marbà, N., Arias-Ortiz, A., Masqué, P., Kendrick, G. A., Mazarrasa, I., Bastyan, G. R., et al. (2015). Impact of seagrass loss and subsequent revegetation on carbon sequestration and stocks. *J. Ecol.* 103 (2), 296–302. doi: 10.1111/1365-2745.12370
- Martin, B. C., Bougoure, J., Ryan, M. H., Bennett, W. W., Colmer, T. D., Joyce, N. K., et al. (2019). Oxygen loss from seagrass roots coincides with colonisation of sulphide-oxidising cable bacteria and reduces sulphide stress. *ISME J.* 13 (3), 707–719. doi: 10.1038/s41396-018-0308-5
- Mateu-Vicens, G., Box, A., Deudero, S., and Rodriguez, B. (2010). Comparative analysis of epiphytic foraminifera in sediments colonized by seagrass *Posidonia oceanica* and invasive macroalgae *Caulerpa* spp. *J. Foraminiferal Res.* 40 (2), 134–147. doi: 10.2113/gsfjr.40.2.134
- Maxwell, P. S., Eklöf, J. S., van Katwijk, M. M., O'Brien, K. R., de la Torre-Castro, M., Boström, C., et al. (2017). The fundamental role of ecological feedback mechanisms for the adaptive management of seagrass ecosystems—a review. *Biol. Rev.* 92 (3), 1521–1538. doi: 10.1111/brv.12294

- Mazarrasa, I., Marbà, N., Lovelock, C. E., Serrano, O., Lavery, P. S., Fourqurean, J. W., et al. (2015). Seagrass meadows as a globally significant carbonate reservoir. *Biogeosciences* 12 (16), 4993–5003. doi: 10.5194/bg-12-4993-2015
- McKenzie, L. J., Nordlund, L. M., Jones, B. L., Cullen-Unsworth, L. C., Roelfsema, C., and Unsworth, R. K. (2020). The global distribution of seagrass meadows. *Environ. Res. Lett.* 15 (7), 074041. doi: 10.1088/1748-9326/ab7d06
- Mejia, A. Y., Rotini, A., Lacasella, F., Bookman, R., Thaller, M. C., Shem-Tov, R., et al. (2016). Assessing the ecological status of seagrasses using morphology, biochemical descriptors and microbial community analyses. A study in *Halophila stipulacea* (Forsk.) Aschers meadows in the northern Red Sea. *Ecol. Indic.* 60, 1150–1163. doi: 10.1016/j.ecolind.2015.09.014
- Meysman, F. J., Galaktionov, O. S., Gribsholt, B., and Middelburg, J. J. (2006). Bioirrigation in permeable sediments: Advective pore-water transport induced by burrow ventilation. *Limnology Oceanography* 51 (1), 142–156. doi: 10.4319/l.2006.51.1.0142
- Mollica, N. R., Guo, W., Cohen, A. L., Huang, K. F., Foster, G. L., Donald, H. K., et al. (2018). Ocean acidification affects coral growth by reducing skeletal density. *Proc. Natl. Acad. Sci.* 115 (8), 1754–1759. doi: 10.1073/pnas.1712806115
- Olsen, J. L., Rouzé, P., Verhelst, B., Lin, Y. C., Bayer, T., Collen, J., et al. (2016). The genome of the seagrass *Zostera marina* reveals angiosperm adaptation to the sea. *Nature* 530 (7590), 331–335. doi: 10.1038/nature16548
- Oscar, M. A., Barak, S., and Winters, G. (2018). The tropical invasive seagrass, *Halophila stipulacea*, has a superior ability to tolerate dynamic changes in salinity levels compared to its freshwater relative, *Vallisneria americana*. *Front. Plant Sci.* 9, 950. doi: 10.3389/fpls.2018.00950
- Pedersen, O., Borum, J., Duarte, C. M., and Fortes, M. D. (1998). Oxygen dynamics in the rhizosphere of *Cymodocea rotundata*. *Mar. Ecol. Prog. Ser.* 169, 283–288. doi: 10.3354/meps169283
- Pellerin, A., Antler, G., Marietou, A., Turchyn, A. V., and Jørgensen, B. B. (2020). The effect of temperature on sulfur and oxygen isotope fractionation by sulfate reducing bacteria (*Desulfococcus multivorans*). *FEMS Microbiol. Lett.* 367 (9), fnaa061. doi: 10.1093/femsle/fnaa061
- Pellerin, A., Antler, G., Røy, H., Findlay, A., Beulig, F., Scholze, C., et al. (2018). The sulfur cycle below the sulfate-methane transition of marine sediments. *Geochimica Cosmochimica Acta* 239, 74–89. doi: 10.1016/j.gca.2018.07.027
- Piñeiro-Juncal, N., Serrano, O., Mateo, M. A., Diaz-Almela, E., Leiva-Dueñas, C., and Martínez-Cortizas, A. (2022). Review of the physical and chemical properties of seagrass soils. *Geoderma* 428, 116219. doi: 10.1016/j.geoderma.2022.116219
- Pyzik, A. J., and Sommer, S. E. (1981). Sedimentary iron monosulfides: kinetics and mechanism of formation. *Geochimica Cosmochimica Acta* 45 (5), 687–698. doi: 10.1016/0016-7037(81)90042-9
- Rees, C. E. (1973). A steady-state model for sulphur isotope fractionation in bacterial reduction processes. *Geochimica Cosmochimica Acta* 37 (5), 1141–1162. doi: 10.1016/0016-7037(73)90052-5
- Reiss, Z., Hottinger, L., Reiss, Z., and Hottinger, L. (1984). The gulf of aqaba—a rift-shaped depression. *Gulf Aqaba: Ecol. Micropaleontology*, 19–32. doi: 10.1007/978-3-642-69787-6\_3
- Rotini, A., Mejia, A. Y., Costa, R., Migliore, L., and Winters, G. (2017). Ecophysiological plasticity and bacteriome shift in the seagrass *Halophila stipulacea* along a depth gradient in the Northern Red Sea. *Front. Plant Sci.* 7 2015. doi: 10.3389/fpls.2016.02015
- Sansone, F. J., and Martens, C. S. (1982). Volatile fatty acid cycling in organic-rich marine sediments. *Geochimica Cosmochimica Acta* 46 (9), 1575–1589. doi: 10.1016/0016-7037(82)90315-5
- Satoh, Y., and Shigeki, W. (2022). Organic matter composition regulates residual potential of organic carbon of the seagrass *Zostera marina* L. during its decomposition process in seawater. *Mar. Environ. Res.* 182, 105790. doi: 10.1016/j.marenvres.2022.105790
- Scholz, V. V., Brodersen, K. E., Kühl, M., and Koren, K. (2021). Resolving chemical gradients around seagrass roots—A review of available methods. *Front. Mar. Sci.* 8, 771382. doi: 10.3389/fmars.2021.771382
- Schorn, S., Ahmerkamp, S., Bullock, E., Weber, M., Lott, C., Liebecke, M., et al. (2022). Diverse methylophilic methanogenic archaea cause high methane emissions from seagrass meadows. *Proc. Natl. Acad. Sci.* 119 (9), e2106628119. doi: 10.1073/pnas.2106628119
- Schubert, N., and Demes, K. (2017). Phenotypic plasticity in the marine angiosperm *Halophila decipiens* (Hydrocharitaceae, Streptophyta). *Marine Ecology Progress Series* 575, 81–93.
- Sela-Adler, M., Ronen, Z., Herut, B., Antler, G., Vigderovich, H., Eckert, W., et al. (2017). Co-existence of methanogenesis and sulfate reduction with common substrates in sulfate-rich estuarine sediments. *Front. Microbiol.* 8, 766. doi: 10.3389/fmicb.2017.00766
- Sharon, Y., Silva, J., Santos, R., Runcie, J. W., Chernihovsky, M., and Beer, S. (2009). Photosynthetic responses of *Halophila stipulacea* to a light gradient. II. Acclimations following transplantation. *Aquat. Biol.* 7 (1-2), 153–157. doi: 10.3354/ab00148
- Short, F. T., Carruthers, T., Dennison, W., and Waycott, M. (2007). Global seagrass distribution and diversity: a bioregional model. *J. Exp. Mar. Biol. Ecol.* 350 (1-2), 3–20. doi: 10.1016/j.jembe.2007.06.012
- Short, F. T., Kosten, S., Morgan, P. A., Malone, S., and Moore, G. E. (2016). Impacts of climate change on submerged and emergent wetland plants. *Aquat. Bot.* 135, 3–17. doi: 10.1016/j.aquabot.2016.06.006
- Sim, M. S., Bosak, T., and Ono, S. (2011a). Large sulfur isotope fractionation does not require disproportionation. *Science* 333 (6038), 74–77. doi: 10.1126/science.1205103
- Sim, M. S., Ono, S., Donovan, K., Templar, S. P., and Bosak, T. (2011b). Effect of electron donors on the fractionation of sulfur isotopes by a marine *Desulfovibrio* sp. *Geochimica Cosmochimica Acta* 75 (15), 4244–4259. doi: 10.1016/j.gca.2011.05.021
- Soetaert, K., Hofmann, A. F., Middelburg, J. J., Meysman, F. J., and Greenwood, J. (2007). Reprint of “The effect of biogeochemical processes on pH”. *Mar. Chem.* 106 (1-2), 380–401. doi: 10.1016/j.marchem.2007.06.008
- Sogin, E. M., Michellod, D., Gruber-Vodicka, H. R., Bourceau, P., Geier, B., Meier, D. V., et al. (2022). Sugars dominate the seagrass rhizosphere. *Nat. Ecol. Evol.* 6 (7), 866–877. doi: 10.1038/s41559-022-01740-z
- Stam, M. C., Mason, P. R., Laverman, A. M., Pallud, C., and Van Cappellen, P. (2011). 34S/32S fractionation by sulfate-reducing microbial communities in estuarine sediments. *Geochimica Cosmochimica Acta* 75 (14), 3903–3914. doi: 10.1016/j.gca.2011.04.022
- Stambler, N. (2006). Light and picophytoplankton in the gulf of Eilat (Aqaba). *J. Geophysical Research: Oceans* 111 (C11). doi: 10.1029/2005JC003373
- Stookey, L. L. (1970). Ferrozine—a new spectrophotometric reagent for iron. *Analytical Chem.* 42 (7), 779–781.
- Ugarelli, K., Chakrabarti, S., Laas, P., and Stingl, U. (2017). The seagrass holobiont and its microbiome. *Microorganisms* 5 (4), 81. doi: 10.3390/microorganisms5040081
- Unsworth, R. K., Collier, C. J., Henderson, G. M., and McKenzie, L. J. (2012). Tropical seagrass meadows modify seawater carbon chemistry: implications for coral reefs impacted by ocean acidification. *Environ. Res. Lett.* 7 (2), 024026. doi: 10.1088/1748-9326/7/2/024026
- Van Der Heide, T., Govers, L. L., De Fouw, J., Olf, H., van der Geest, M., Van Katwijk, M. M., et al. (2012). A three-stage symbiosis forms the foundation of seagrass ecosystems. *science* 336 (6087), 1432–1434. doi: 10.1126/science.1219973
- van de Velde, S. J., Hidalgo-Martinez, S., Callebaut, I., Antler, G., James, R. K., Leermakers, M., et al. (2020). Burrowing fauna mediate alternative stable states in the redox cycling of salt marsh sediments. *Geochimica Cosmochimica Acta* 276, 31–49. doi: 10.1016/j.gca.2020.02.021
- Wada, S., Satoh, Y., and Hama, T. (2022). Massive loss and microbial decomposition in reproductive biomass of *Zostera marina*. *Estuarine, Coastal and Shelf Science* 275, 107986.
- Waldron, K. W., Baydoun, E. A. H., and Brett, C. T. (1989). Comparison of cell wall composition of tissues from the seagrasses *Halophila* and *Halodule*. *Aquat. Bot.* 35 (2), 209–218. doi: 10.1016/0304-3770(89)90106-X
- Wang, F., and Chapman, P. M. (1999). Biological implications of sulfide in sediment—a review focusing on sediment toxicity. *Environ. Toxicol. Chemistry: Int. J.* 18 (11), 2526–2532. doi: 10.1002/etc.5620181120
- Waycott, M., Duarte, C. M., Carruthers, T. J., Orth, R. J., Dennison, W. C., Olyarnik, S., et al. (2009). Accelerating loss of seagrasses across the globe threatens coastal ecosystems. *Proc. Natl. Acad. Sci.* 106 (30), 12377–12381. doi: 10.1073/pnas.0905620106
- Wing, B. A., and Halevy, I. (2014). Intracellular metabolite levels shape sulfur isotope fractionation during microbial sulfate respiration. *Proc. Natl. Acad. Sci.* 111 (51), 18116–18125. doi: 10.1073/pnas.1407502111
- Winters, G., Beer, S., Willette, D. A., Viana, I. G., Chiquillo, K. L., Beca-Carretero, P., et al. (2020). The tropical seagrass *Halophila stipulacea*: reviewing what we know from its native and invasive habitats, alongside identifying knowledge gaps. *Front. Mar. Sci.* 7, 300. doi: 10.3389/fmars.2020.00300
- Winters, G., Edelist, D., Shem-Tov, R., Beer, S., and Rilov, G. (2017). A low cost field-survey method for mapping seagrasses and their potential threats: An example from the northern Gulf of Aqaba, Red Sea. *Aquat. Conservation: Mar. Freshw. Ecosyst.* 27 (2), 324–339. doi: 10.1002/aqc.2688
- Wortmann, U. G., Bernasconi, S. M., and Boettcher, M. E. (2001). Hypersulfidic deep biosphere indicates extreme sulfur isotope fractionation during single-step microbial sulfate reduction. *Geology* 29 (7), 647–650. doi: 10.1130/0091-7613(2001)029<0647:HDBIES>2.0.CO;2